Introduction: collective modes and exotic nuclei

Muhsin N. Harakeh

KVI-CART, Groningen

Workshop on "Collective Mode Study through Beta-Decay Measurements"
SUBATECH, Nantes;19-20 January 2015

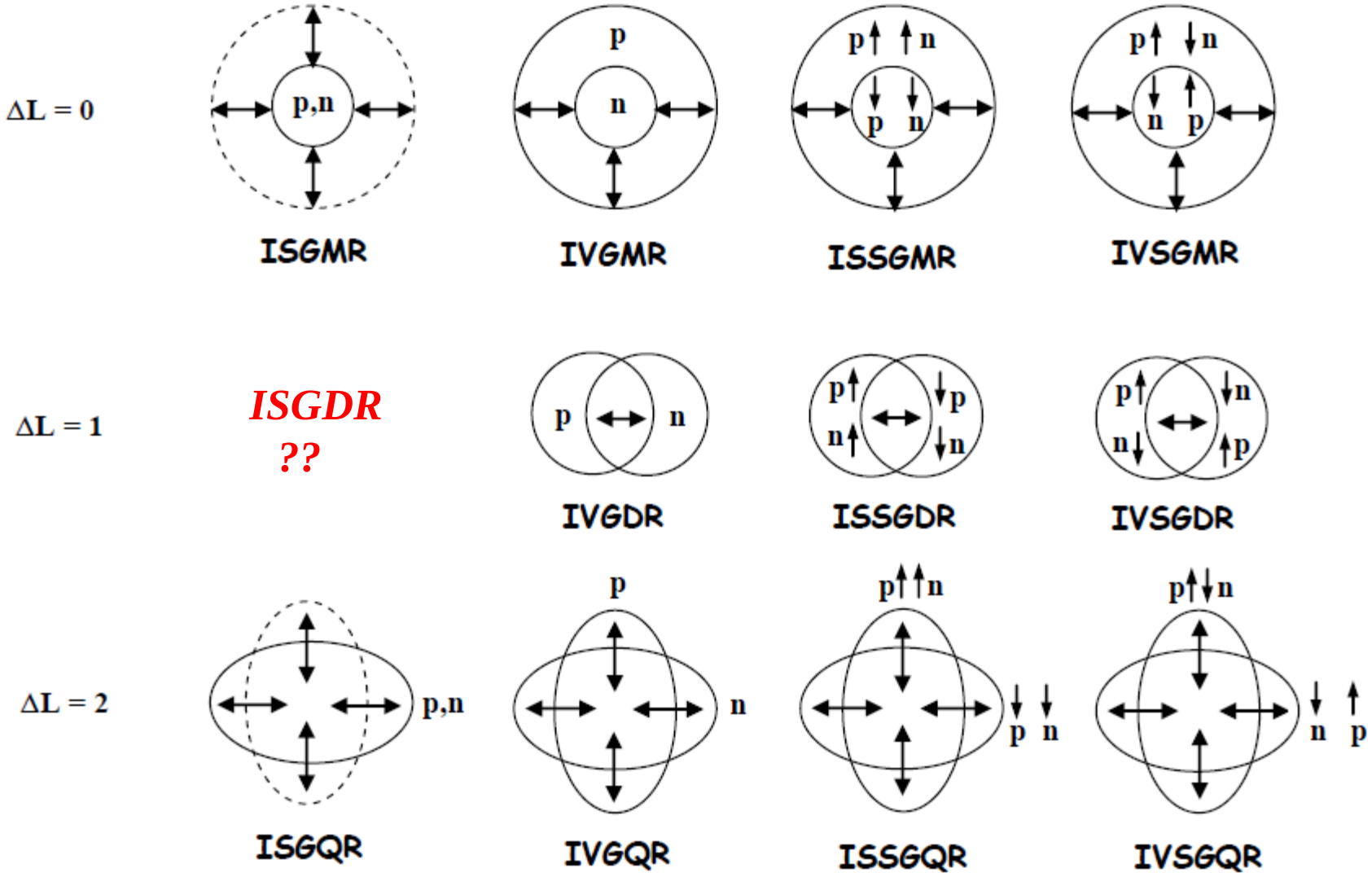
ΔL = 0
p,n
ISGMR
p
n
IVGMR
p↑ ↑n
p ↑ n ↑
ISSGMR
p↑ ↓n
n ↓ p ↑
IVSGMR
ΔL = 1
ISGDR
??
p
n
IVGDR
p↑ p↓
n↑ n↓
ISSGDR
p↑ n↓
n↓ p↑
IVSGDR
ΔL = 2
p,n
ISGQR
p
n
IVGQR
p↑↑n
p↓ n↑
ISSGQR
p↑↓n
n↓ p↑
IVSGQR
ΔT = 0
ΔS = 0
ΔT = 1
ΔS = 0
ΔT = 0
ΔS = 1
ΔT = 1
ΔS = 1

Microscopic picture: GRs are coherent (1p-1h) excitations induced by single-particle operators.

- **Excitation energy depends on**

  ***i*) multipole *L* (*L*ħω, since radial operator ∝ r^L; except for ISGMR and ISGDR, 2ħω & 3ħω, respectively),**

  ***ii*) strength of effective interaction and**

  ***iii*) collectivity.**

- **Exhaust appreciable % of EWSR**
- **In addition to Landau damping, they acquire a width due to coupling to continuum and to underlying 2p-2h configurations.**

Nucleus → **Many-body system with a finite size**

Vibrations → **Multipole expansion with r, Y_{lm}, τ, σ**

	ΔS=0, ΔT=0	ΔS=0, ΔT=1	ΔS=0, ΔT=1	ΔS=1, ΔT=1	ΔS=1, ΔT=1
L=0: Monopole	ISGMR r^2Y_0	IAS τY_0	IVGMR τr^2Y_0	GTR $\tau\sigma Y_0$	IVSGMR $\tau\sigma r^2Y_0$
L=1: Dipole	ISGDR $(r^3 - 5/3\langle r^2\rangle r)Y_1$		IVGDR τrY_1		IVSGDR $\tau\sigma rY_1$
L=2: Quadrupole	ISGQR r^2Y_2		IVGQR τr^2Y_2		IVSGQR $\tau\sigma r^2Y_2$
L=3: Octupole	LEOR, HEOR r^3Y_3				

$\Delta N = 1$ **E1 (IVGDR)**

$\Delta N = 2$ **E2 (ISGQR)**

&

$\Delta N = 0$ **E0 (ISGMR)**

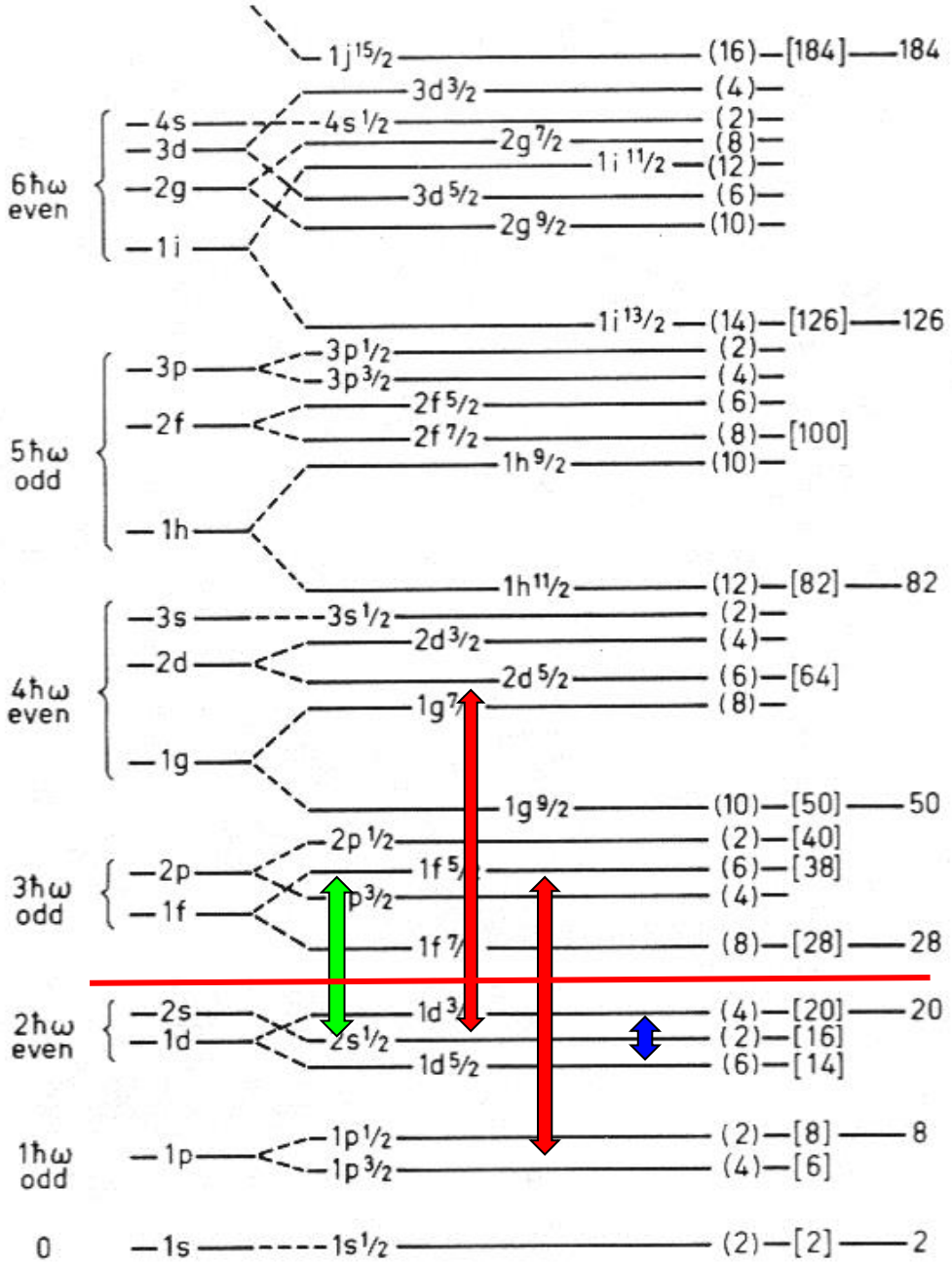

The collective response of the nucleus
Giant Resonances

Electric giant resonances

Isoscalar

Isovector

Monopole (GMR)

Dipole (GDR)

Quadrupole (GQR)

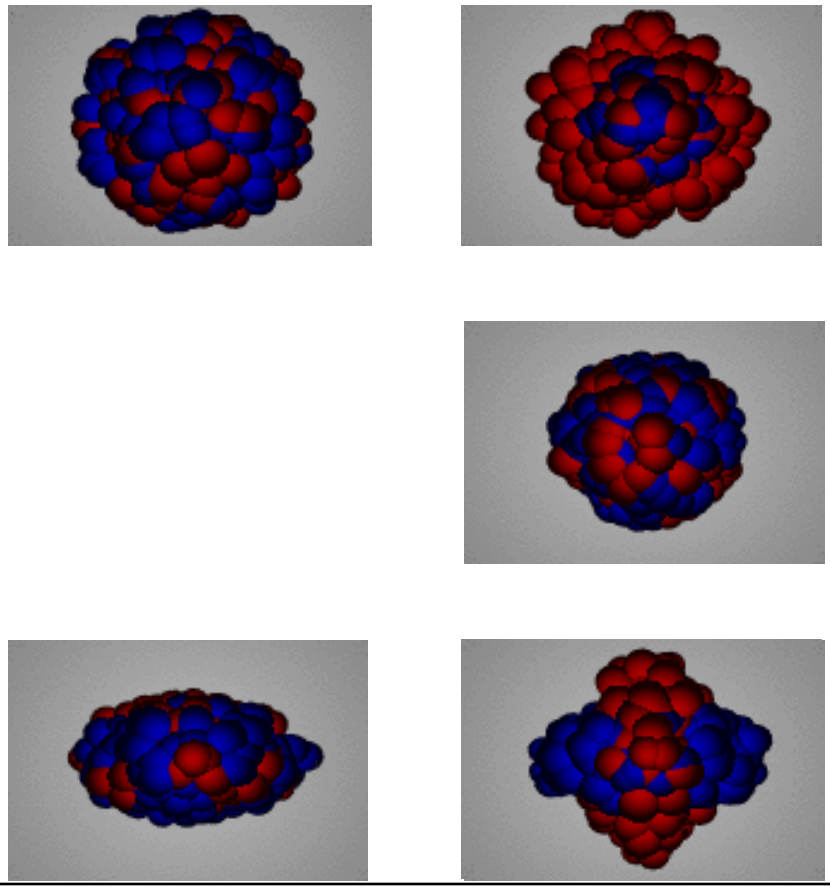

Photo-neutron cross sections

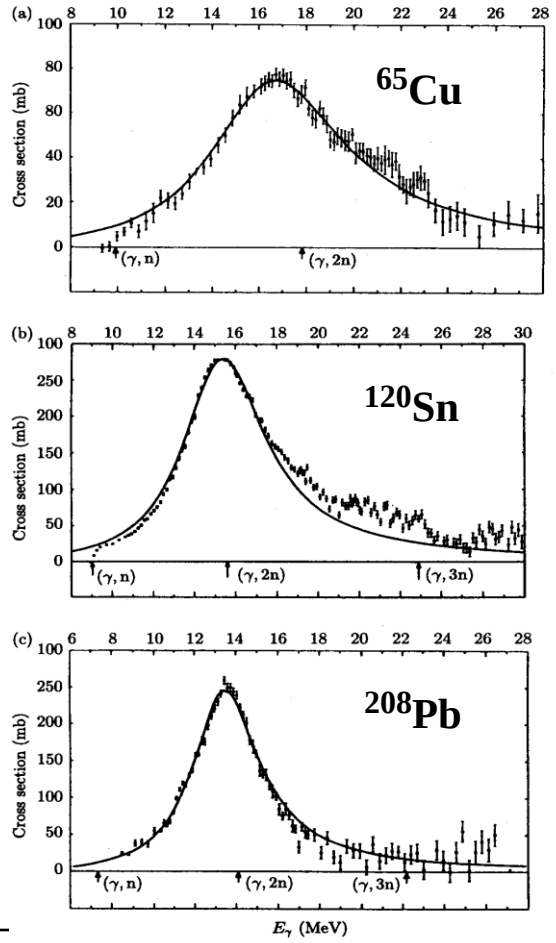

Berman and Fultz, Rev. Mod. Phys. 47 (1975) 47

Spin-isospin excitations

Neutral (ν,ν') and charged (ν_e,e^-), (ν_e,e^+) currents

NC $\Rightarrow$ Inelastic electron and proton scattering

$\Rightarrow$ M0, M1, M2

CC $\Rightarrow$ Charge-exchange reactions

Isovector charge-exchange modes

$\Rightarrow$ IAS, GTR, IVSGMR, IVSGDR, etc.

Importance for nuclear astrophysics,

ν-physics, 2β-decay, n-skin thickness, etc.

(p,n), (^{3}He,t) {GT$^-$}; (n,p), (d,^{2}He) & (t,^{3}He) {GT$^+$}

Charge-exchange probes

(*p*,*n*)-type ($\Delta T_z = -1$)

- β^--decay
- (*p*,*n*)
- (^{3}He,*t*)
- heavy ion

(*n*,*p*)-type ($\Delta T_z = +1$)

- β^+-decay
- (*n*,*p*)
- (*d*,^{2}He)
- (*t*,^{3}He)
- heavy ion; (^{7}Li,^{7}Be)

- Energy per nucleon (>100 MeV/u)
- Spin-flip versus non-spin-flip
- Complexity of reaction mechanism
- Experimental considerations

Spin-isospin excitations

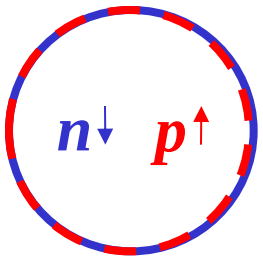

ΔL=0 ΔS=1 ΔT=1
GTR

- **Gamow-Teller transitions;**
  Isospin (ΔT=1); Spin (ΔS=1)

Advantages

- **Cross section peaks at**
  θ = 0° (ΔL=0)
- **Strong excitation of GT states at E/A=100-500 MeV/u**

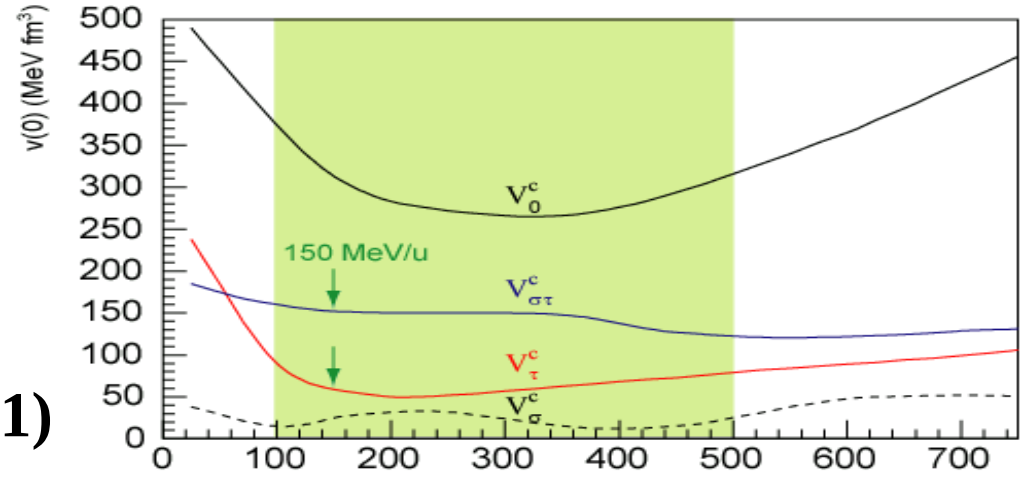

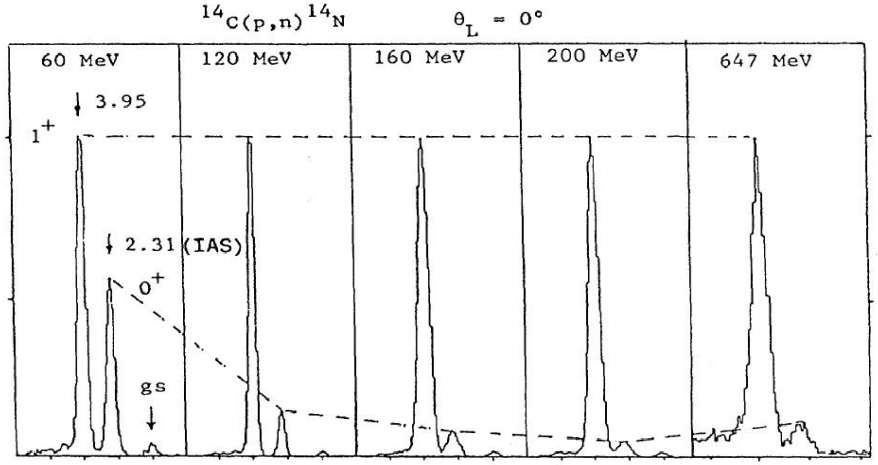

FIG. 4. Zero-degree cross-section spectra for the $^{14}C(p,n)^{14}N$ reactions at the indicated bombarding energies. The spectra have been arbitrarily normalized. From Gaarde (1985) and Rapaport (1989).

⇒ **At RCNP, Osaka**

E(^{3}He) ≈ 150 MeV/u

Spin-flip & GT transitions

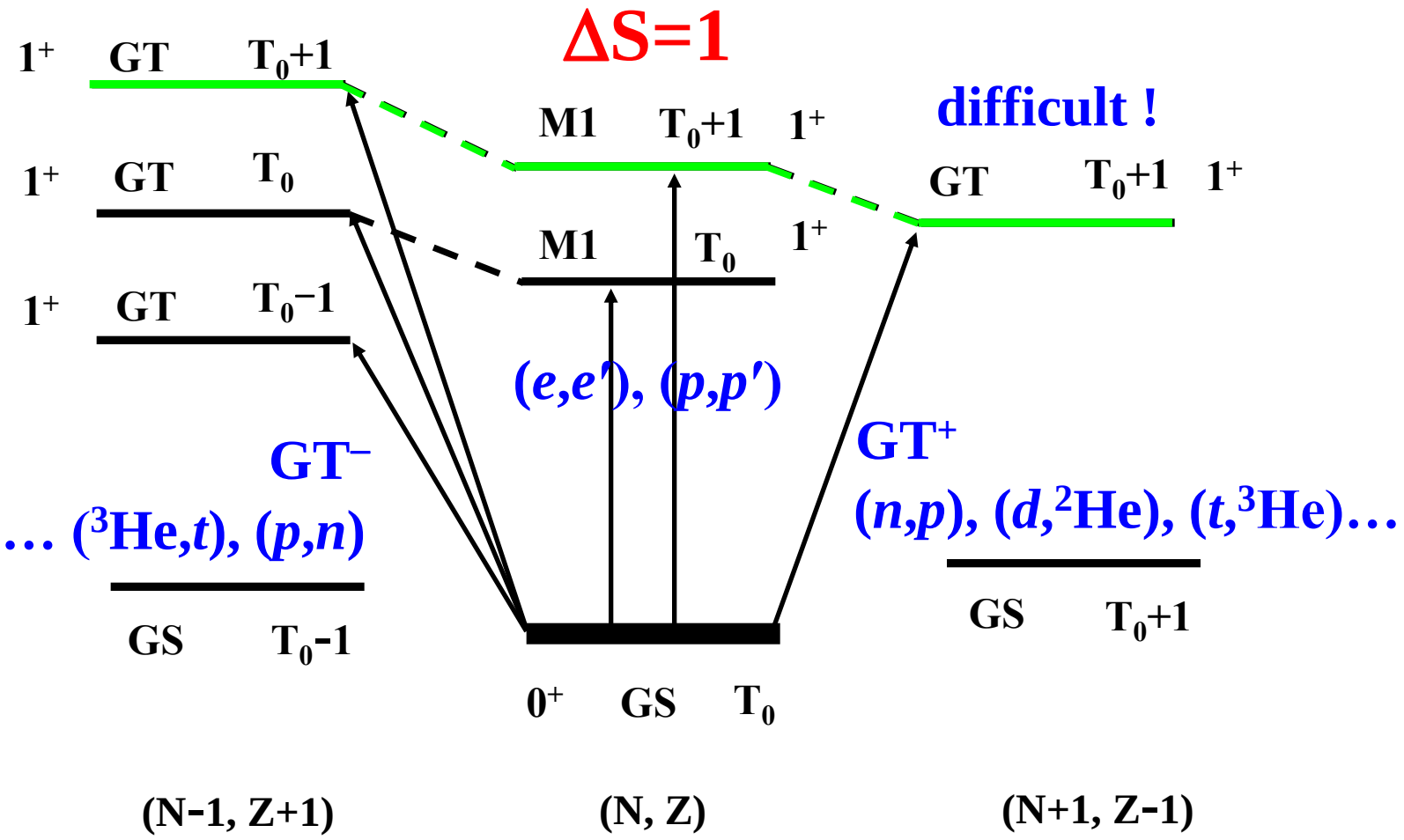

The (^{3}He,t) reaction at 0 degree

- **Cross sections at E(^{3}He)=450 MeV, q=0 for (^{3}He,t) reactions**

$$\frac{d\sigma}{d\Omega} = \frac{\mu_i \mu_f}{(\pi\hbar^2)^2}\left(\frac{k_f}{k_i}\right)(N_\tau^D \mid J_\tau \mid^2 B(F) + N_{\sigma\tau}^D \mid J_{\sigma\tau} \mid^2 B(GT))$$

T. N. Taddeucci *et al.*, Nucl. Phys. A469, 125 (1987)
I. Bergqvist *et al.*, Nucl. Phys. A469, 648 (1987)

- **Neutrino absorption cross sections**

$$\sigma = \frac{1}{\pi \hbar^4 c^3}\left[G_V^2 B(F) + G_A^2 B(GT)\right] \times F(Z, E_e) p_e E_e$$

***F*(*Z*, E_e) is the relativistic Coulomb barrier factor**

Importance of charge-exchange reactions at intermediate energies

Experiments

- **RCNP facility**

  K=400 MeV ring cyclotron

  Grand Raiden spectrometer

- **Beam: $^{3}He^{++}$, 450 MeV**

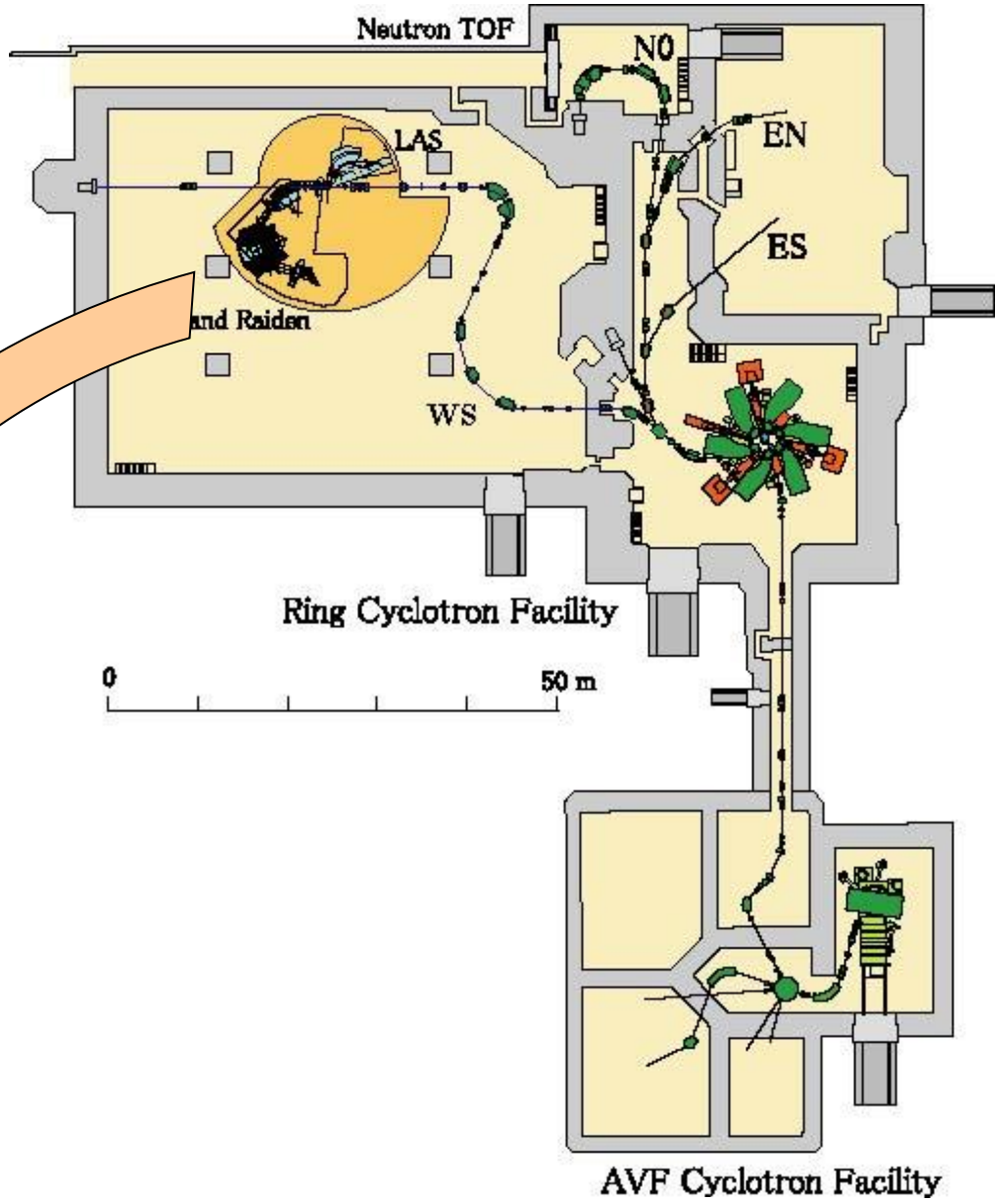

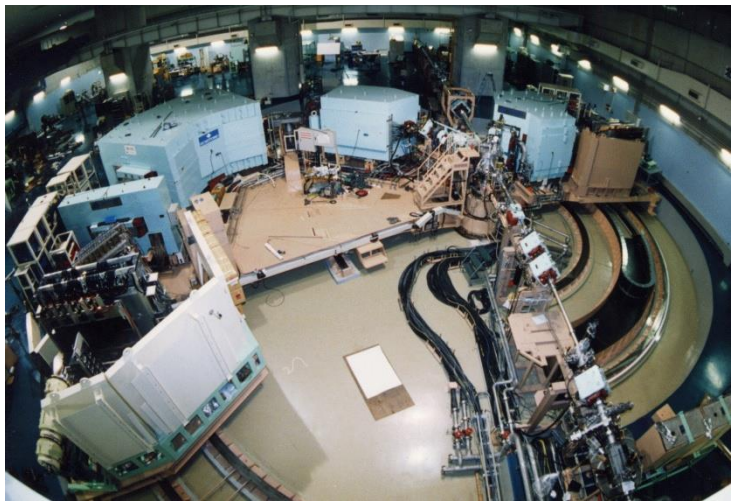

M. Fujiwara *et al.*, NIM A422 (1999) 484

Beam line WS-course

Grand-Raiden Spectrometer

M. Fujiwara *et al.*, NIM A422 (1999) 484

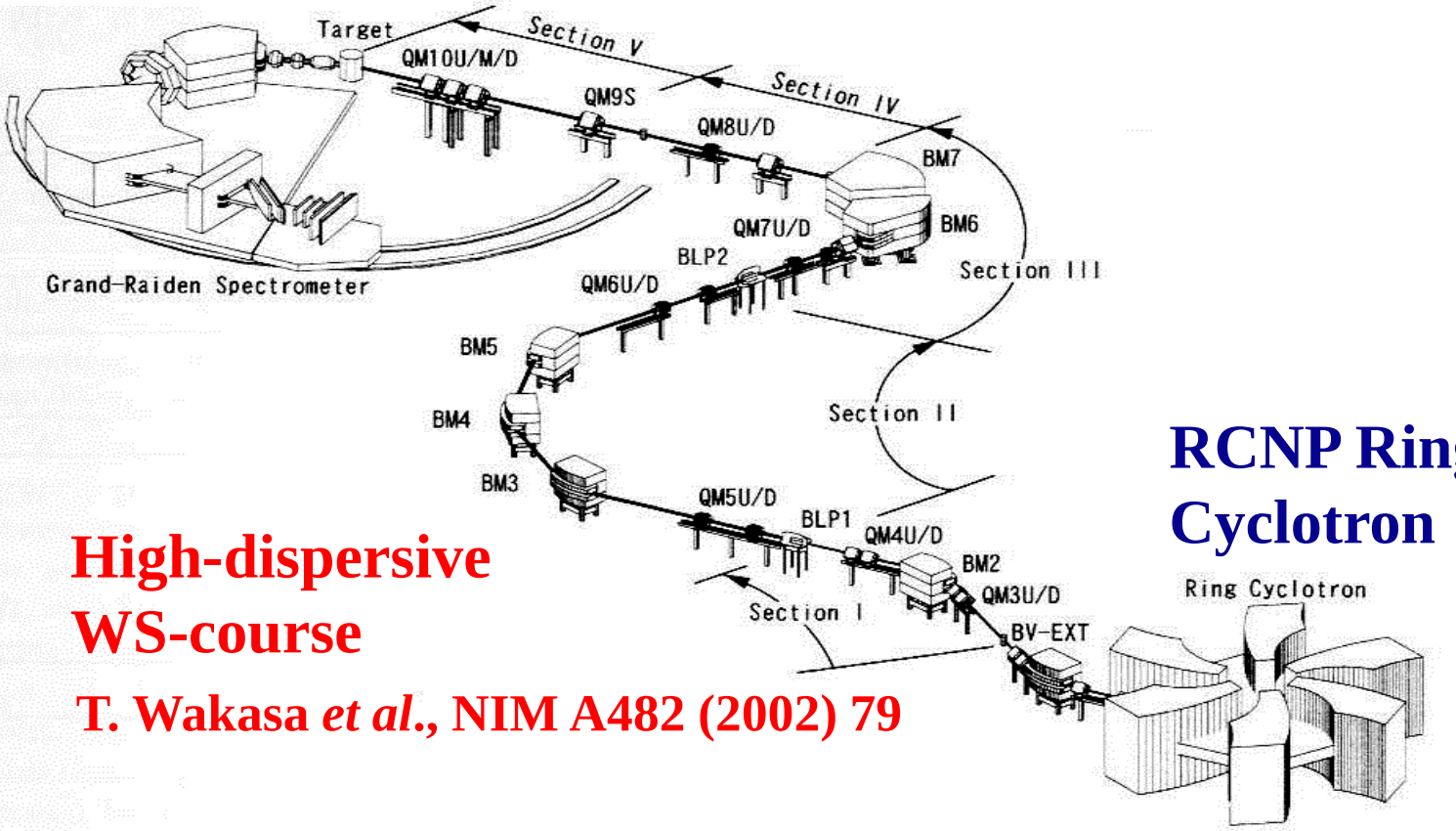

RCNP Ring Cyclotron

High-dispersive WS-course

T. Wakasa *et al.*, NIM A482 (2002) 79

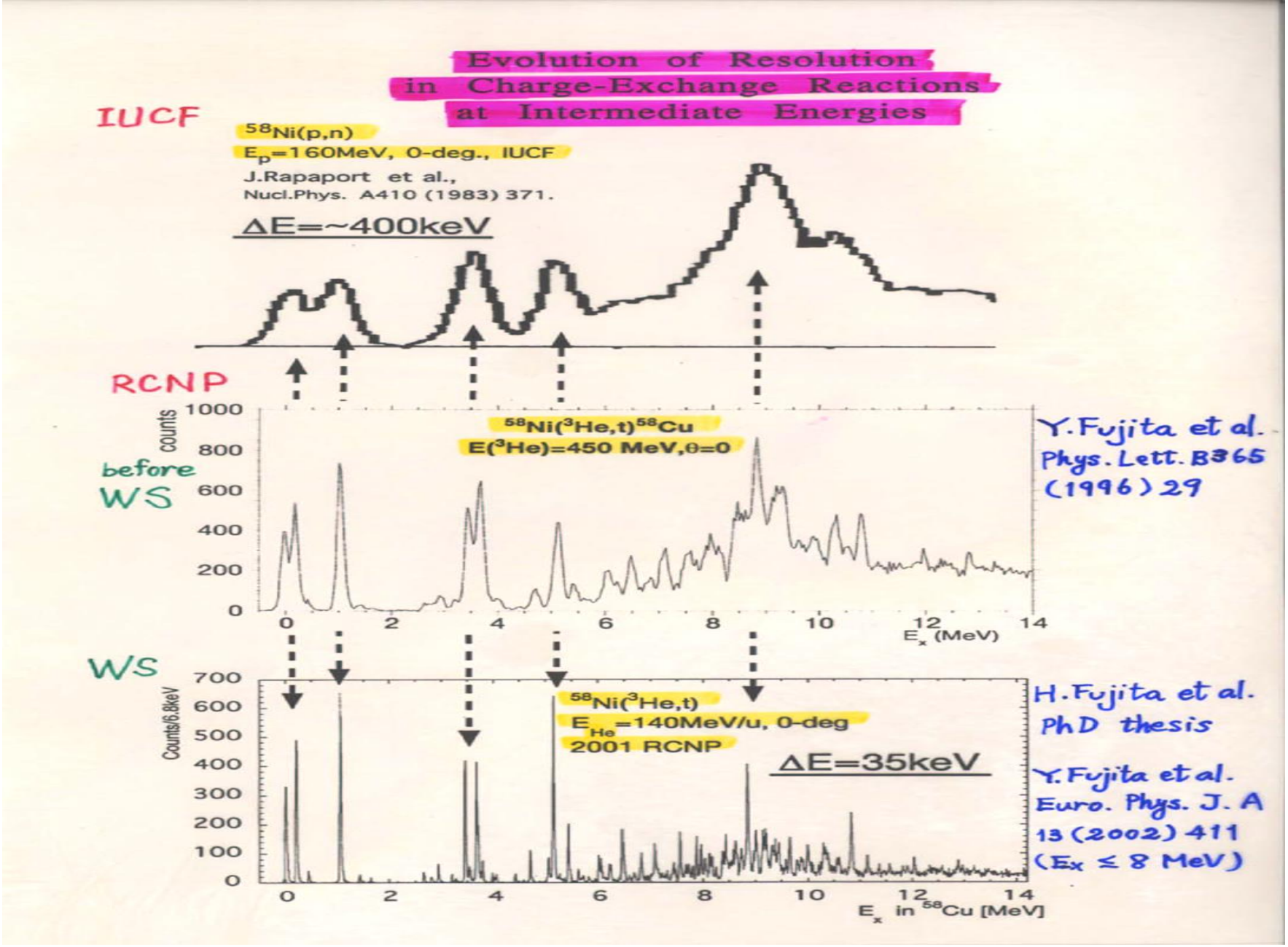
Evolution of Resolution in Charge-Exchange Reactions at Intermediate Energies
IUCF
58Ni(p,n)
Ep=160MeV, 0-deg., IUCF
J.Rapaport et al.,
Nucl.Phys. A410 (1983) 371.
ΔE=~400keV
RCNP
before WS
58Ni(3He,t)58Cu
E(3He)=450 MeV,θ=0
counts
Ex (MeV)
Y.Fujita et al.
Phys.Lett. B365 (1996) 29
WS
58Ni(3He,t)
EHe=140MeV/u, 0-deg
2001 RCNP
ΔE=35keV
Counts/6.8keV
Ex in 58Cu [MeV]
H.Fujita et al.
PhD thesis
Y.Fujita et al.
Euro. Phys. J. A 13 (2002) 411
(Ex ≤ 8 MeV)

^{26}Mg(p,n)^{26}Al & ^{26}Mg(^{3}He,t)^{26}Al spectra

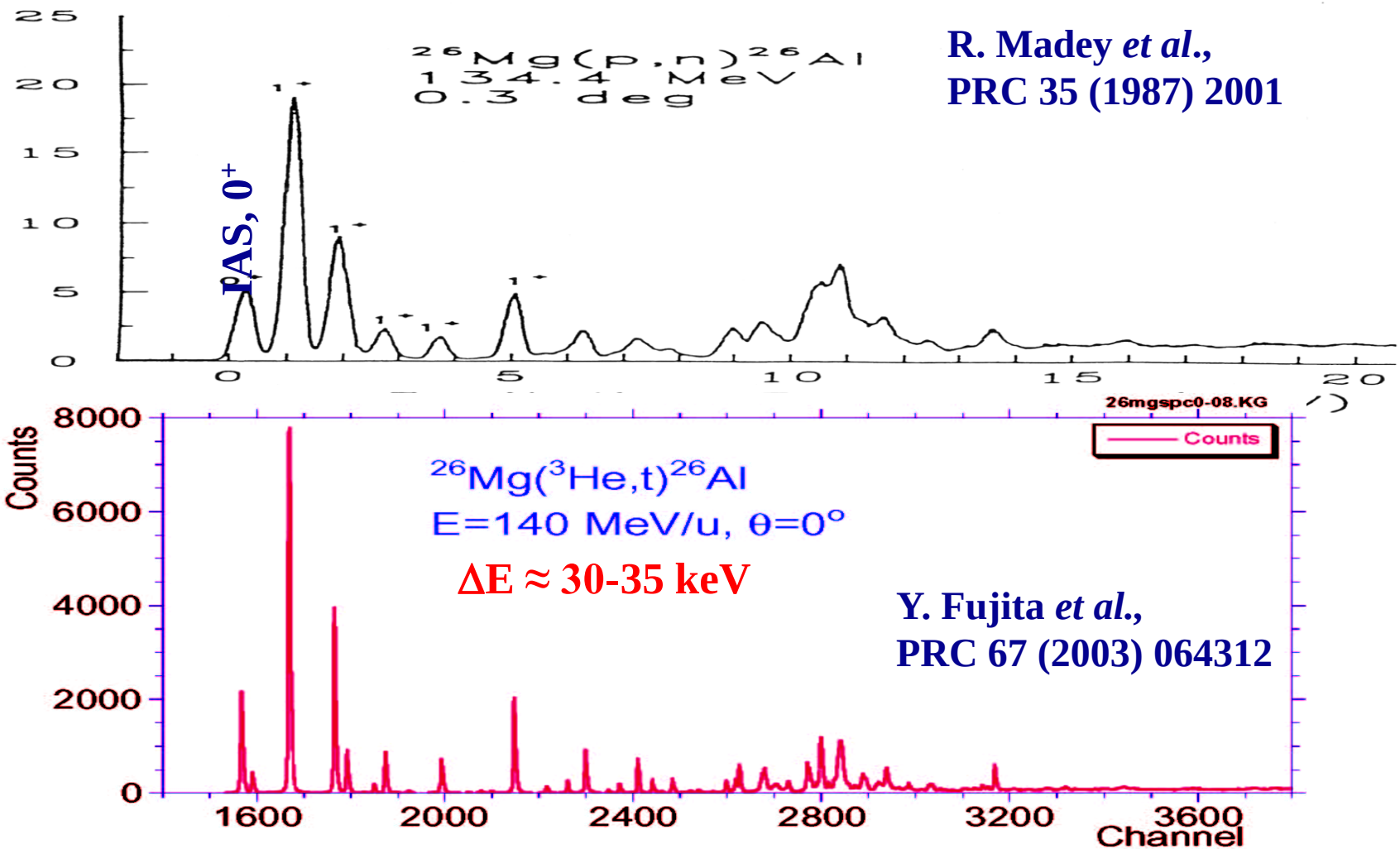

R. Madey *et al.*,
PRC 35 (1987) 2001

Y. Fujita *et al.*,
PRC 67 (2003) 064312

Prominent states are GT states and the IAS !

^{54}Fe(p,n) & ^{54}Fe(^{3}He,t)

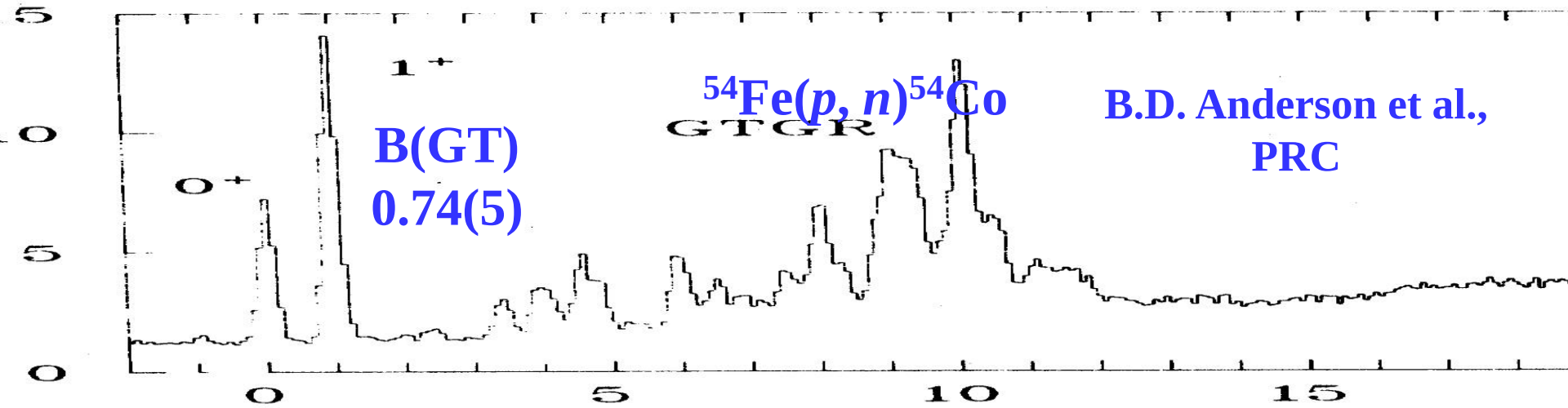

B(GT)
0.74(5)

^{54}Fe(p, n)^{54}Co

B.D. Anderson et al., PRC

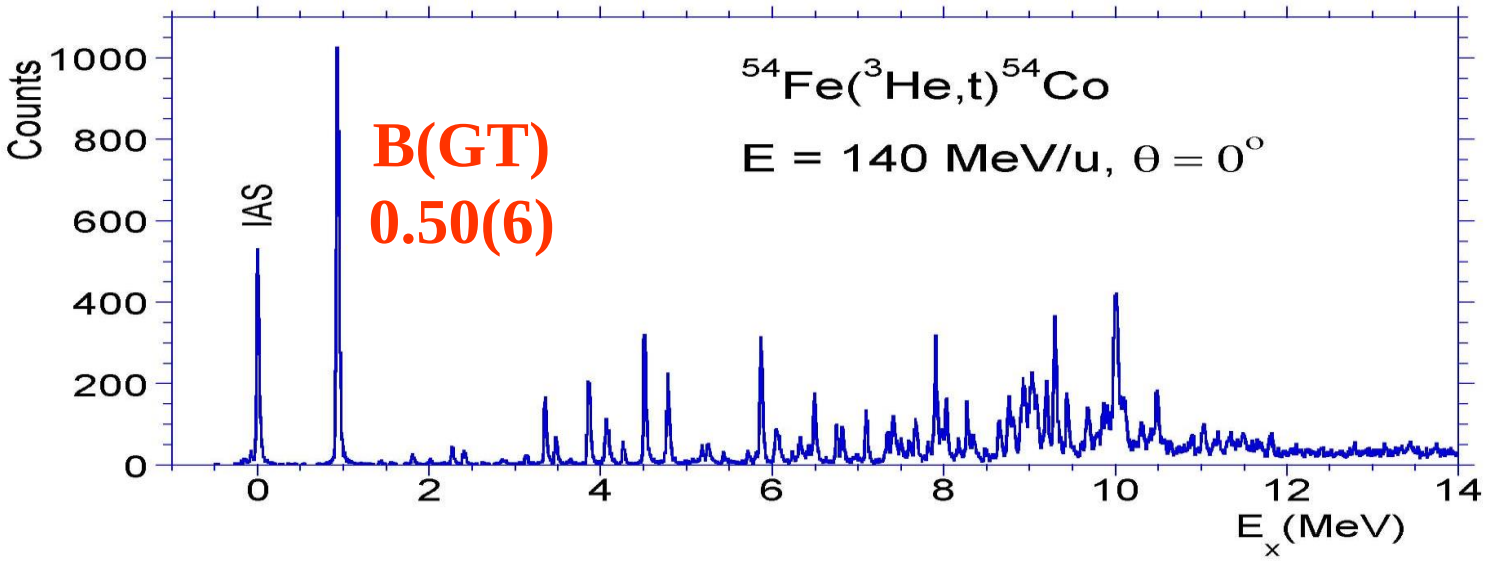

B(GT)
0.50(6)

^{136}Xe(^{3}He,*t*)^{136}Cs

E(^{3}He) = 420 MeV

ΔE = 42 keV

$$B_{exp}(GT+) = \frac{d\sigma(q=0)}{d\Omega} \cdot \left[\frac{d\hat{\sigma}(GT)}{d\Omega}\right]^{-1}$$

extrapolated (DWBA)

unit cross section

ΔL = 2 & ΔL = 0 incoherent

P. Puppe *et al.*, PRC 84 (2011) 051305(R)

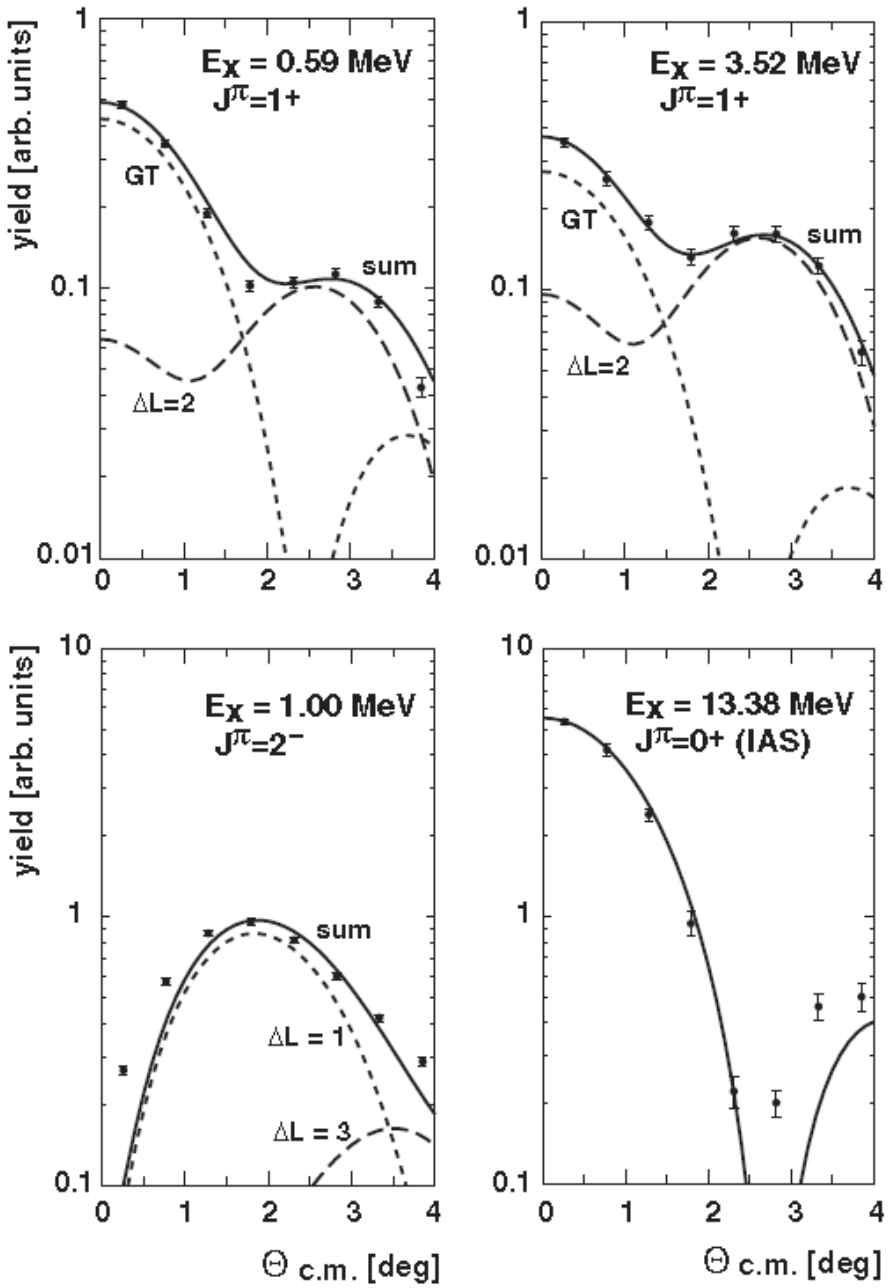

(^{3}He,*t*) charge-exchange reaction on all stable Sn nuclei at IUCF, Bloomington
E(^{3}He) =200 MeV
Excitation energy spectra are plotted relative to IAS.

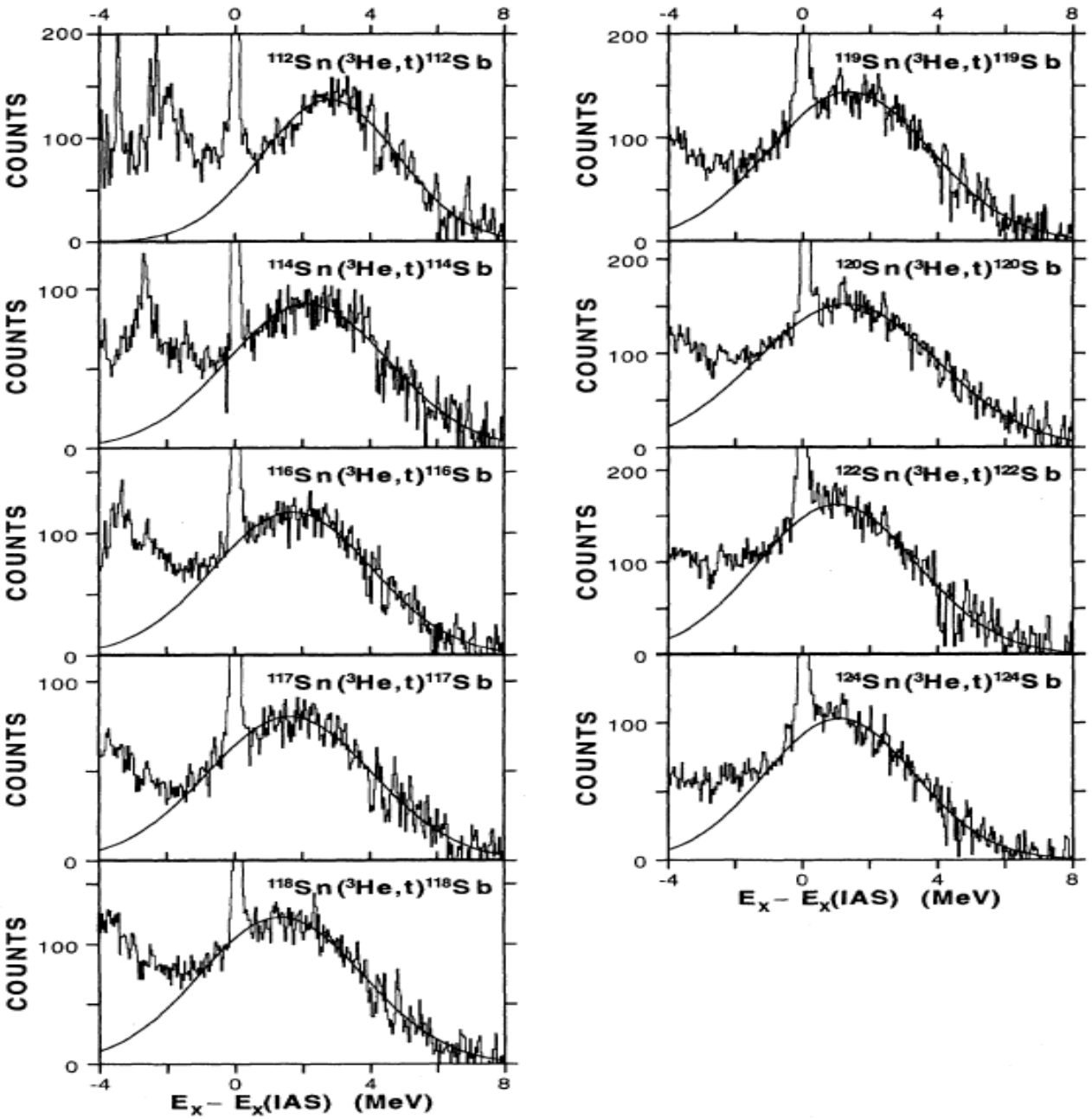

K. Pham *et al.*, PRC **51** (1995) 526

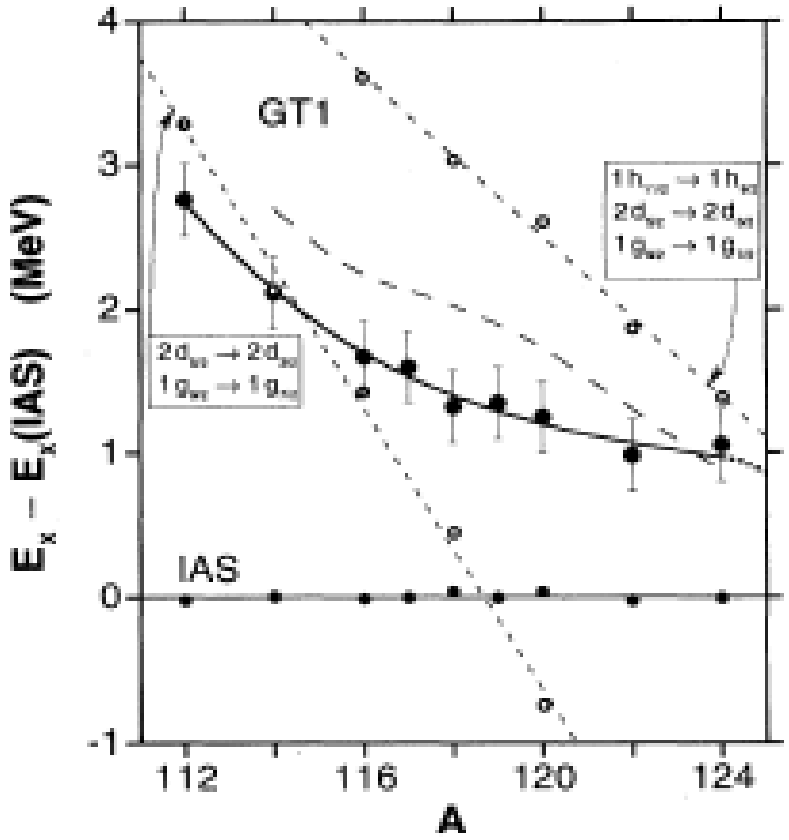

Excitation energy of main component of GTGR relative to IAS.

K. Pham *et al.*, PRC **51** (1995) 526

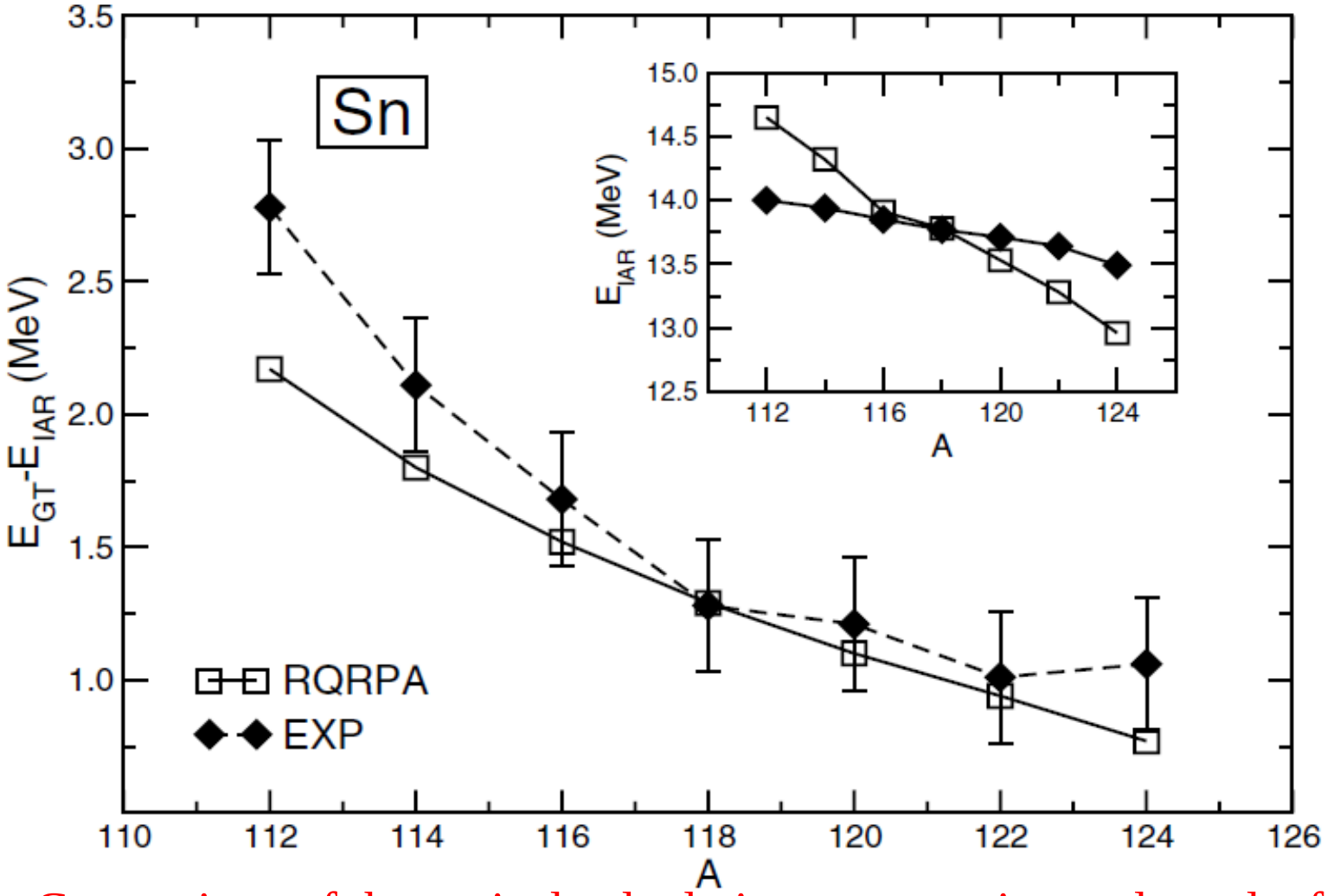

Comparison of theoretical calculations to experimental results for excitation energy of main component of GTGR relative to IAS. Inset shows IAS energies

D. Vretenar *et al.*, PRL **91** (2003) 262502

Theoretical pn-RQRPA and experimental differences of GTGR and IAS excitation energies as function of neutron-skin thickness (data from K. Pham). Lower panel shows comparison between theoretical neutron-skin thickness and experimental data (data from A. Krasznahorkay).

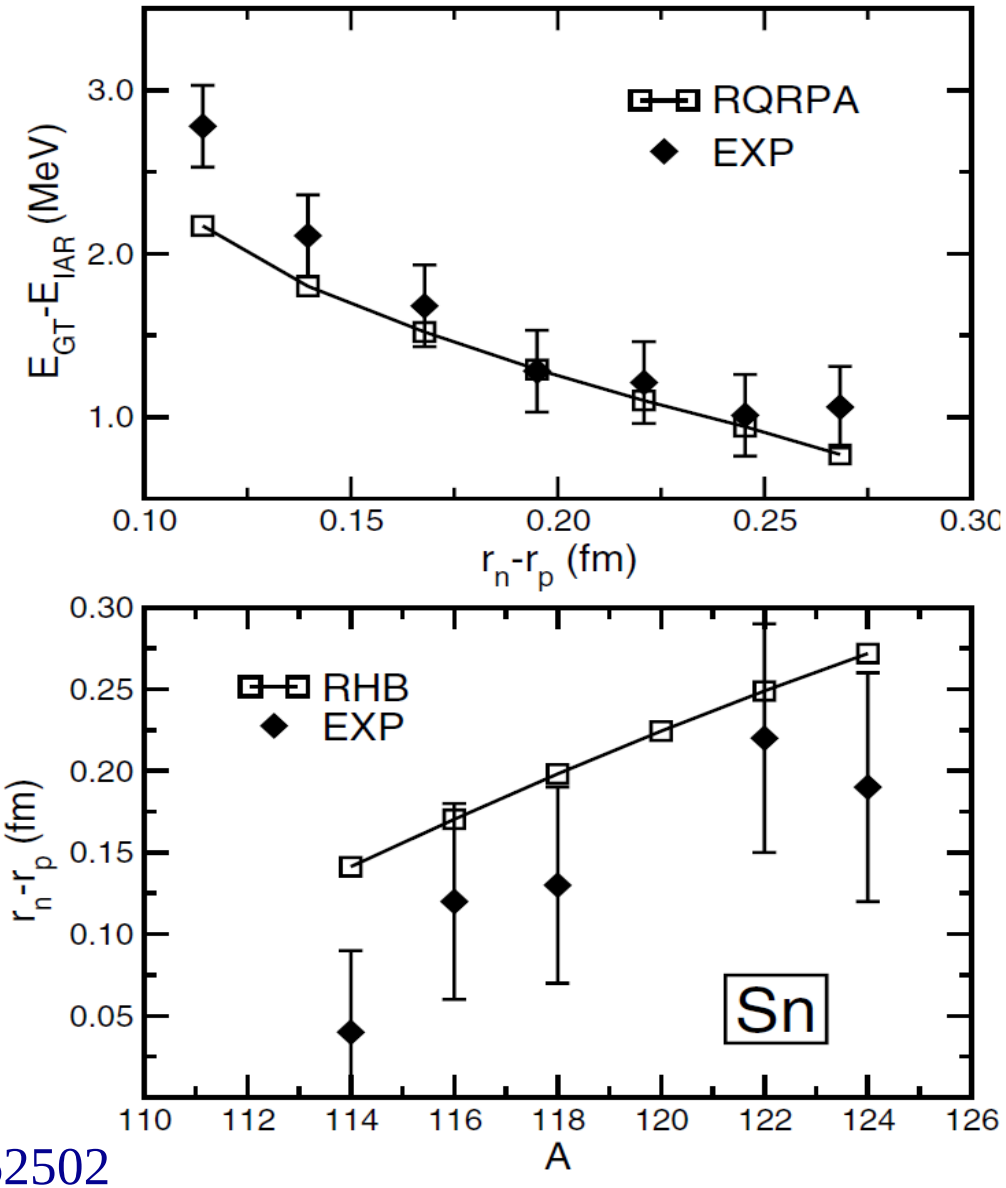

D. Vretenar *et al.*, PRL **91** (2003) 262502

A. Krasznahorkay *et al.*, PRL **83** (1999) 3216; $\mathbf{r_n}$-$\mathbf{r_p}$

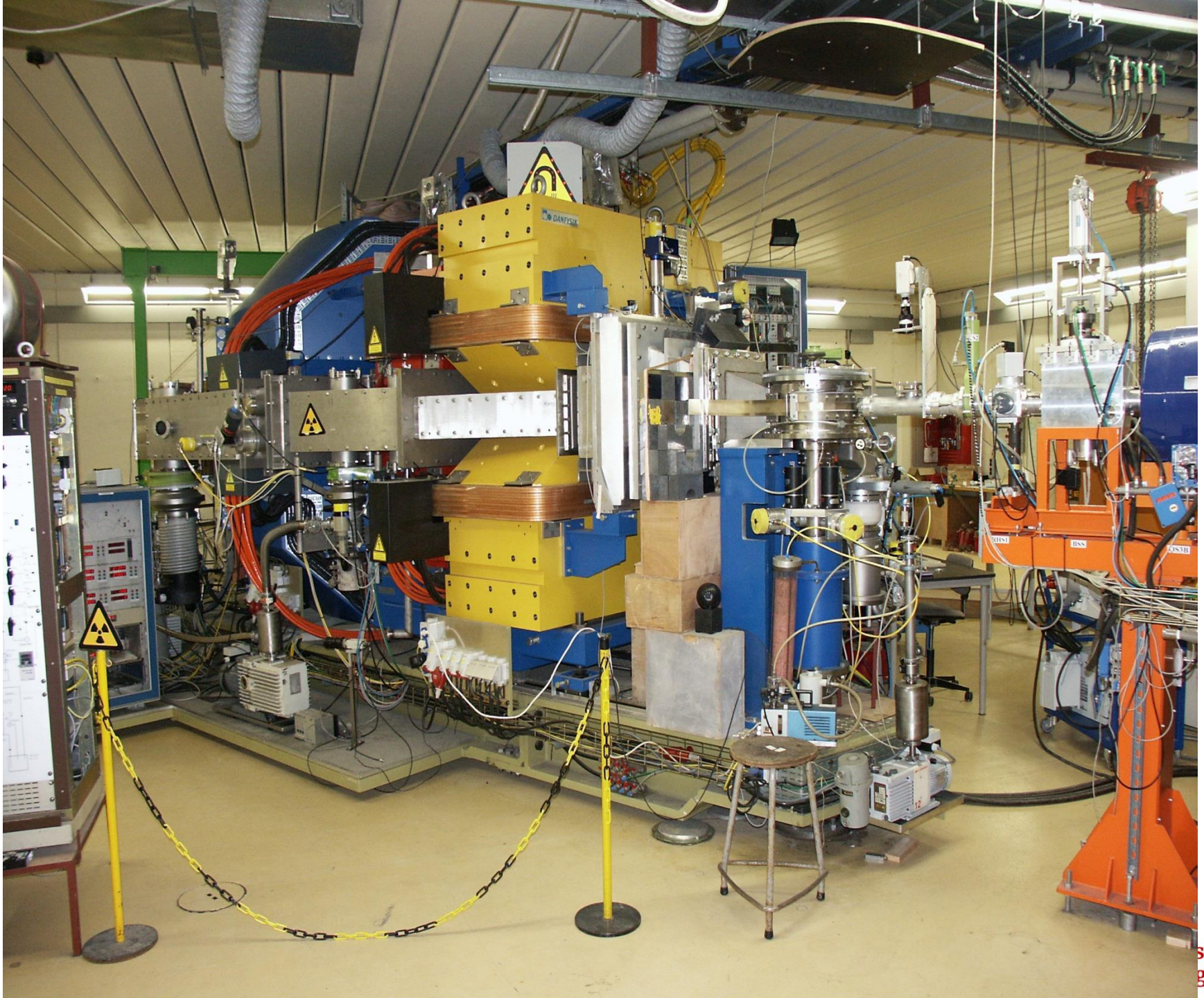
DANFYSIK
BSS
QS3B

fp-shell nuclei: large scale shell model calculations

E. Caurier *et al.*
NPA 653 (1999) 439

- **Stellar weak reaction rates with improved reliability**
- **Large scale shell model (SM) calculations**
- **Tuned to reproduce GT^+ strength measured in (*n*,*p*)**

- **(*n*,*p*) data from TRIUMF**
- **GT^+ strength from SM**
- **Folded with energy resolution**

Case study: ^{58}Ni

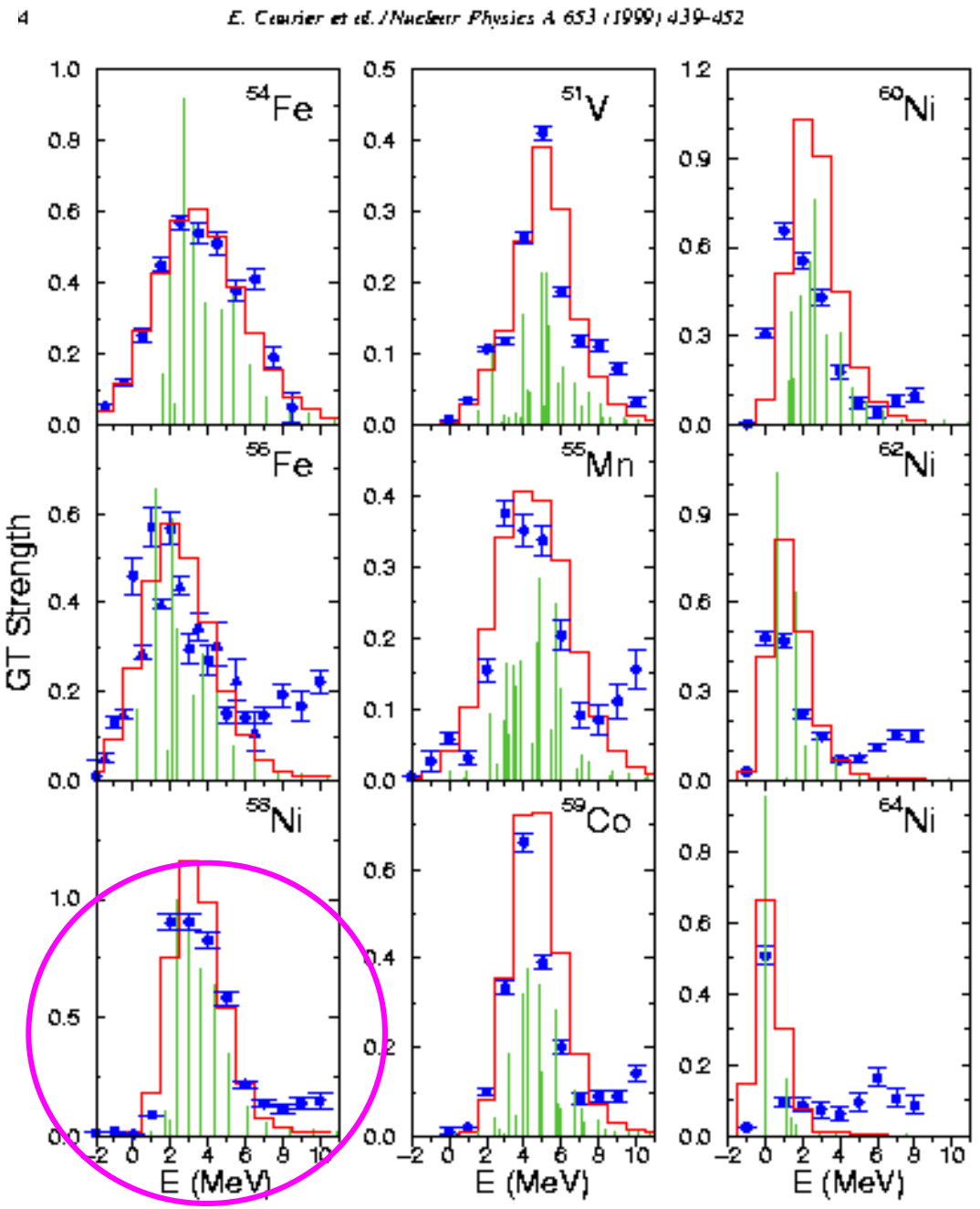

Exclusive excitations ΔS=ΔT=1: (d,^{2}He)

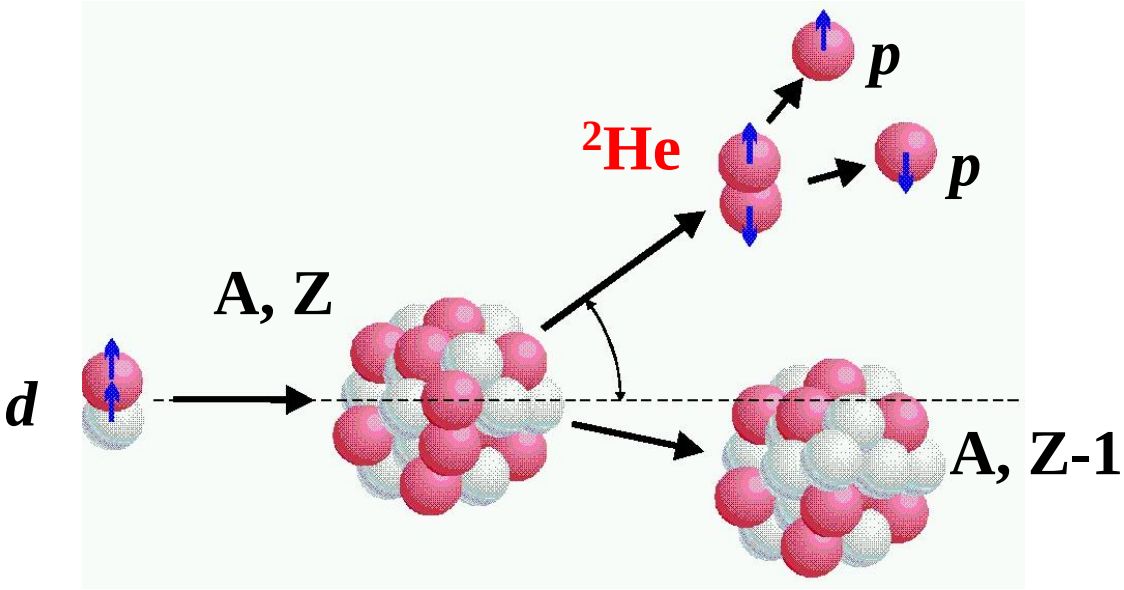

$^3S_1$ deuteron ⇒ $^1S_0$ di-proton (^{2}He)

$^1S_0$ dominates if (relative) 2-proton kinetic energy ε < 1 MeV

(n,p)-type probe with exclusive ΔS=1 character (GT^+ transitions)

But near 0°: tremendous background from d-breakup

(d,^{2}He) as GT$^+$ probe in fp-shell nuclei

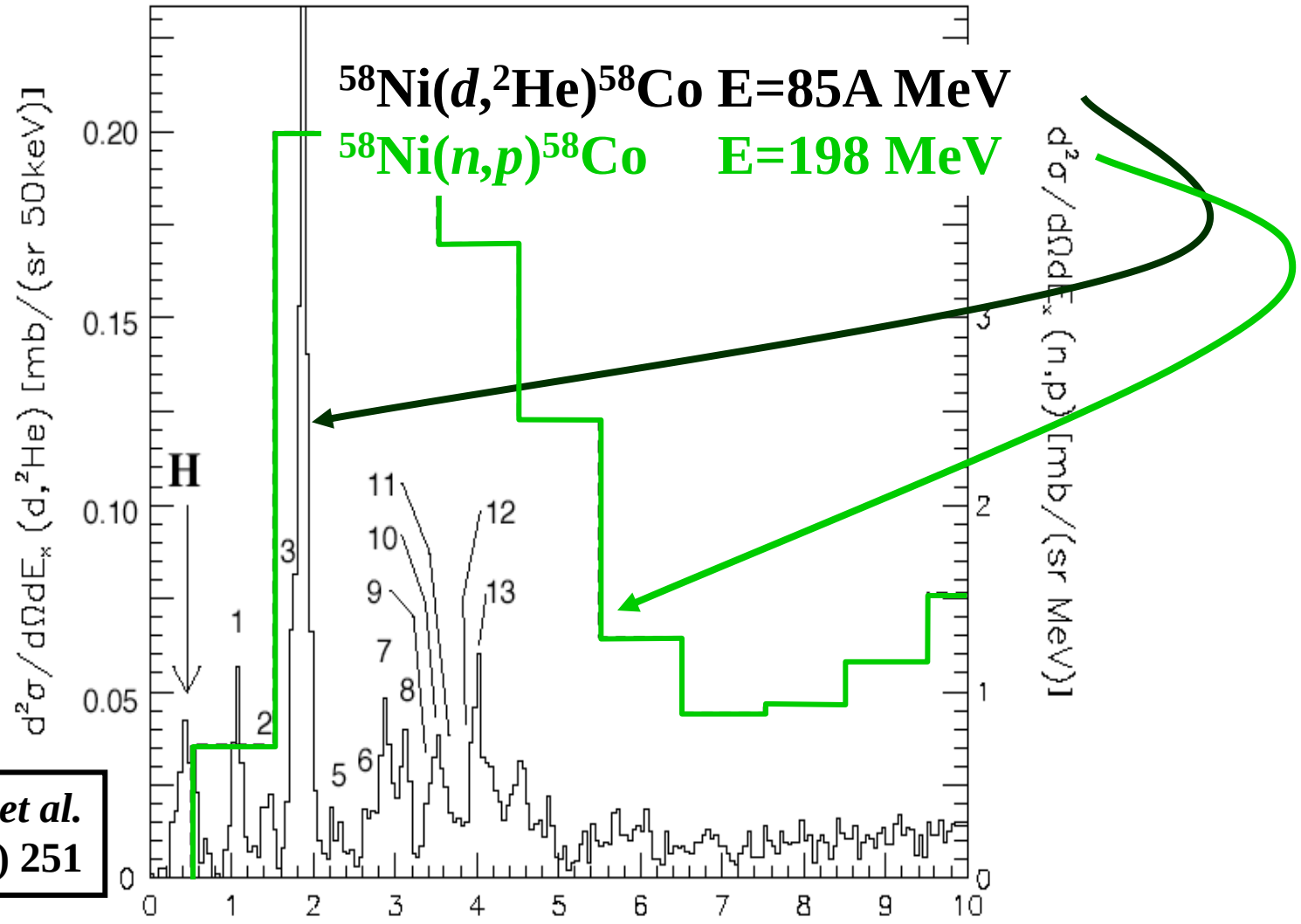

M. Hagemann *et al.*
PLB 579 (2004) 251

Decay scheme of ^{32}Ar.
The limit of detection corresponded to 8.75 MeV excitation in ^{32}CI.

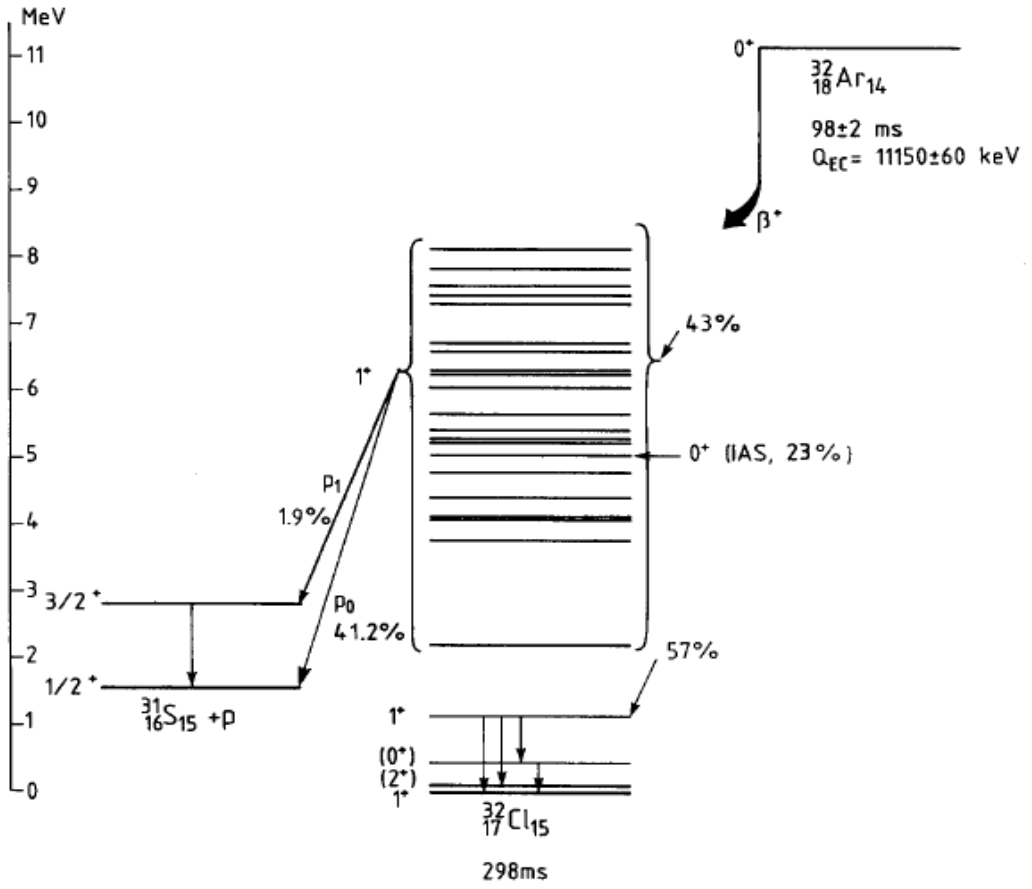

T. Björnstad *et al.*, NPA **443** (1985) 283

The ^{32}Ar Gamow-Teller strength function beta decay and beta-delayed proton decay. The GTR is observed at about 7.5 MeV, in agreement with shell-model predictions by Müller *et al*. [PRC **3** (1971) 700] shown in lower part of the figure. Quenching in the four regions indicated in figure are 0.6, 1.0, 0.5, and 0.4, respectively. The overall renormalization of the axial-vector strength is $(g'_A/g_A)^2=0.49$.

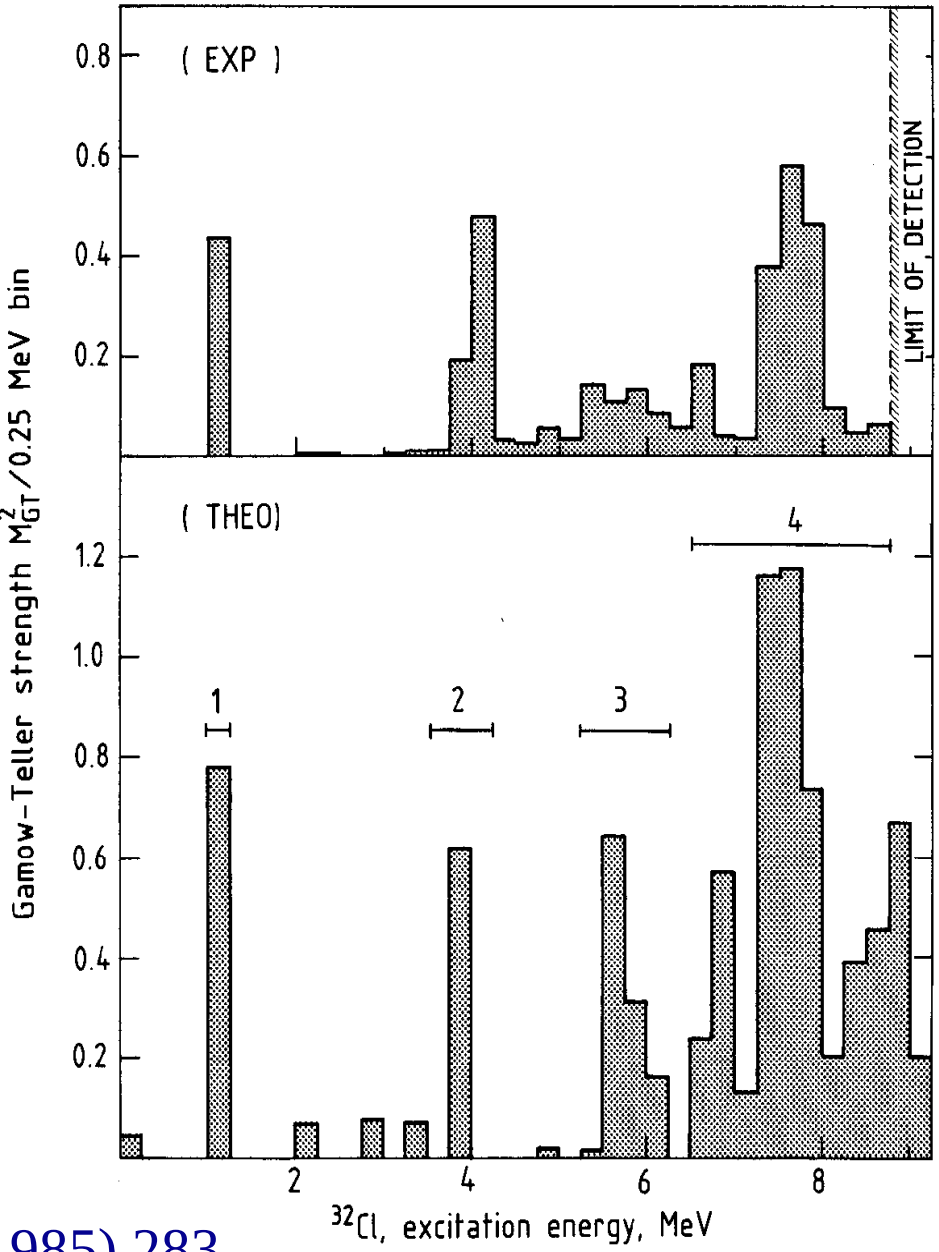

T. Björnstad *et al*., NPA **443** (1985) 283

Hartree-Fock potentials

Dashed: Without Coulomb potential

Solid: With Coulomb potential

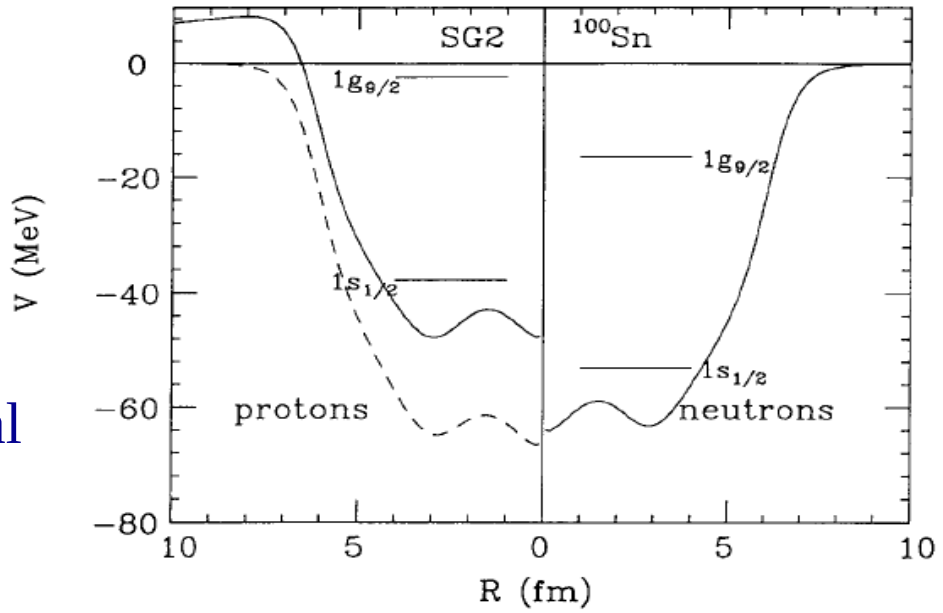

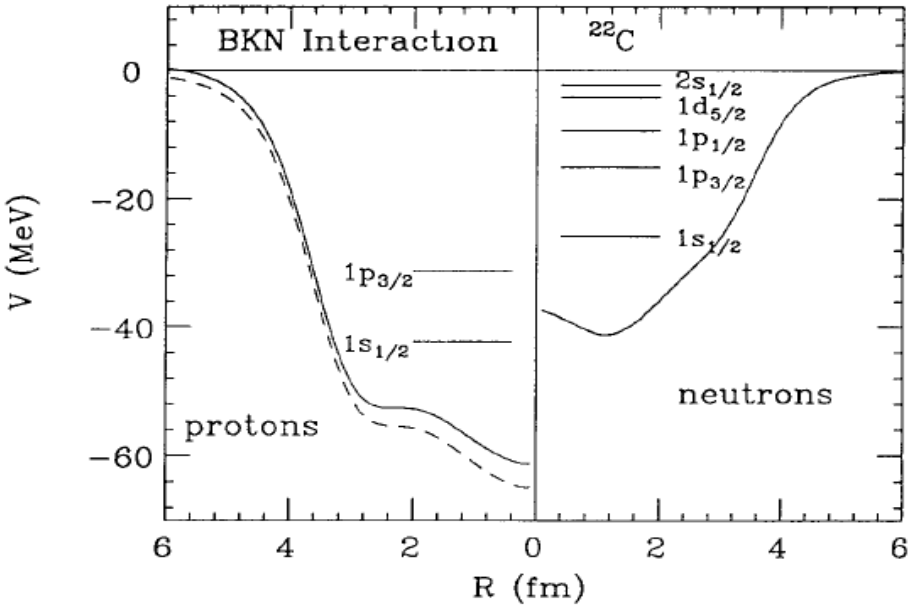

I. Hamamoto & H. Sagawa,
PRC **48** (1993) R960;
I. Hamamoto,
NPA A577 (1994) 19c

I. Hamamoto, NPA A577 (1994) 19c

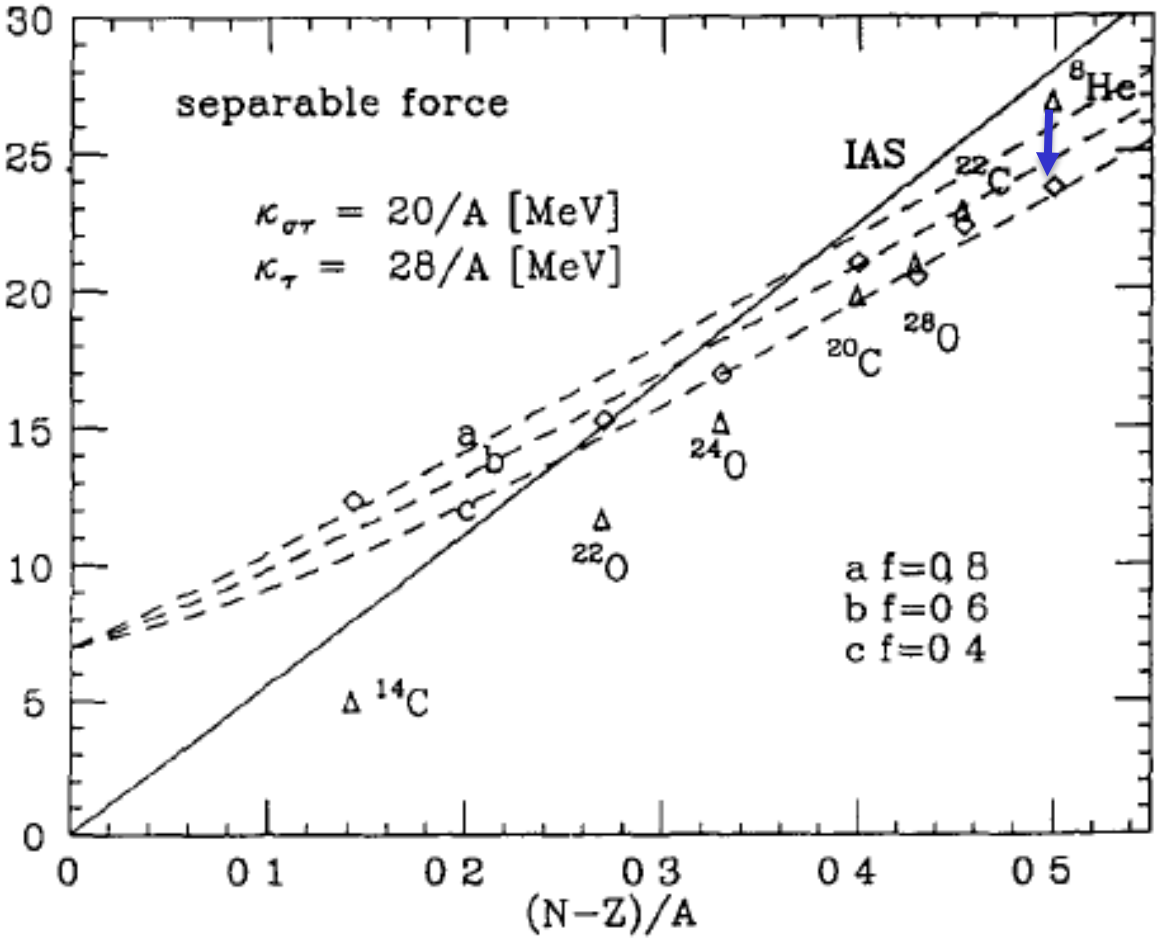

Energies of GTGR (dashed lines) and IAS (solid line) obtained in a schematic model with f the quenching factor of GT strength. Diamonds are GTGR based on mother nuclei and triangles are g.s. of mother nuclei

I. Hamamoto & H. Sagawa, PRC **48** (1993) R960

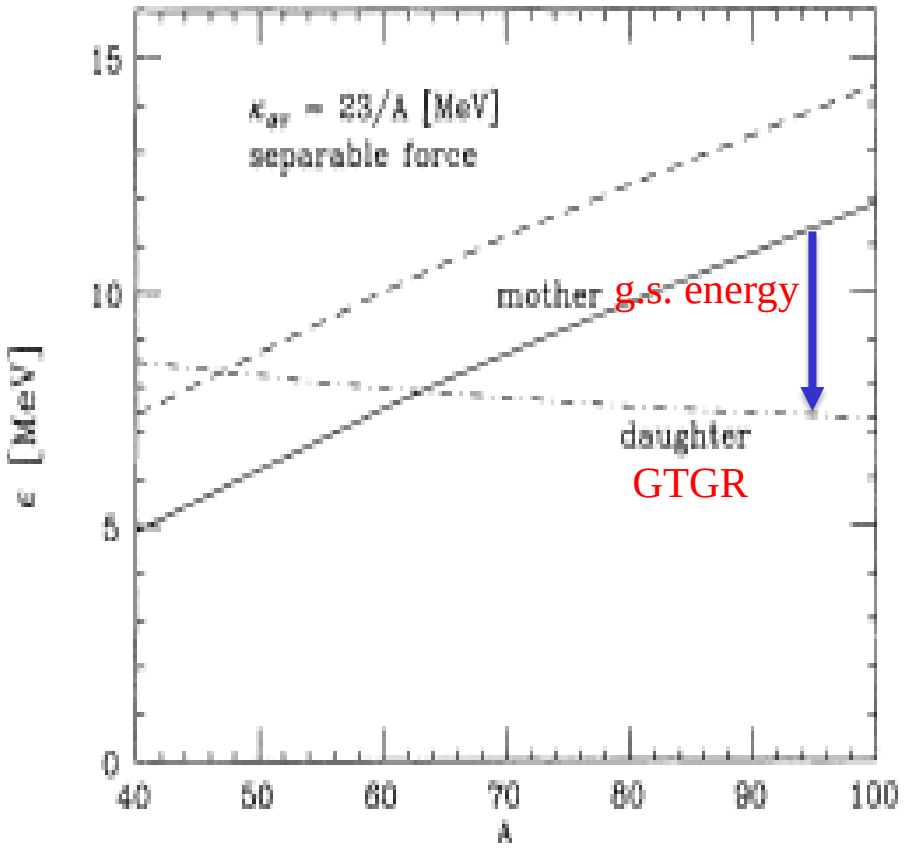

Energies of GTGR (dash-dotted line) of N=Z nuclei calculated in a schematic model.

Dashed (solid) line is energy of mother nucleus without (with) correction term α = 2.5 MeV.

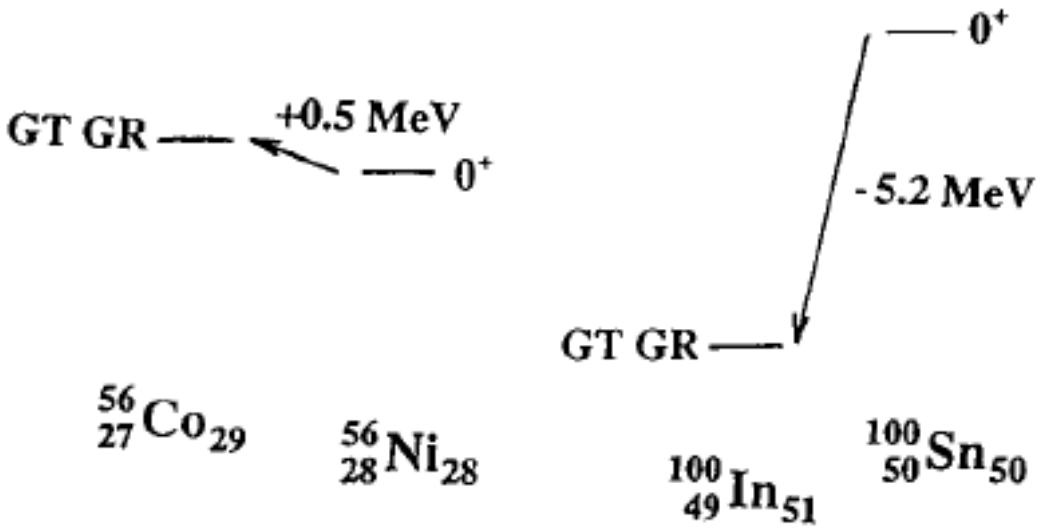

HF-TDA

Energy of GTGR relative to g.s. of *N*=*Z* nuclei

^{56}Ni & ^{100}Sn

I. Hamamoto, NPA A577 (1994) 19c

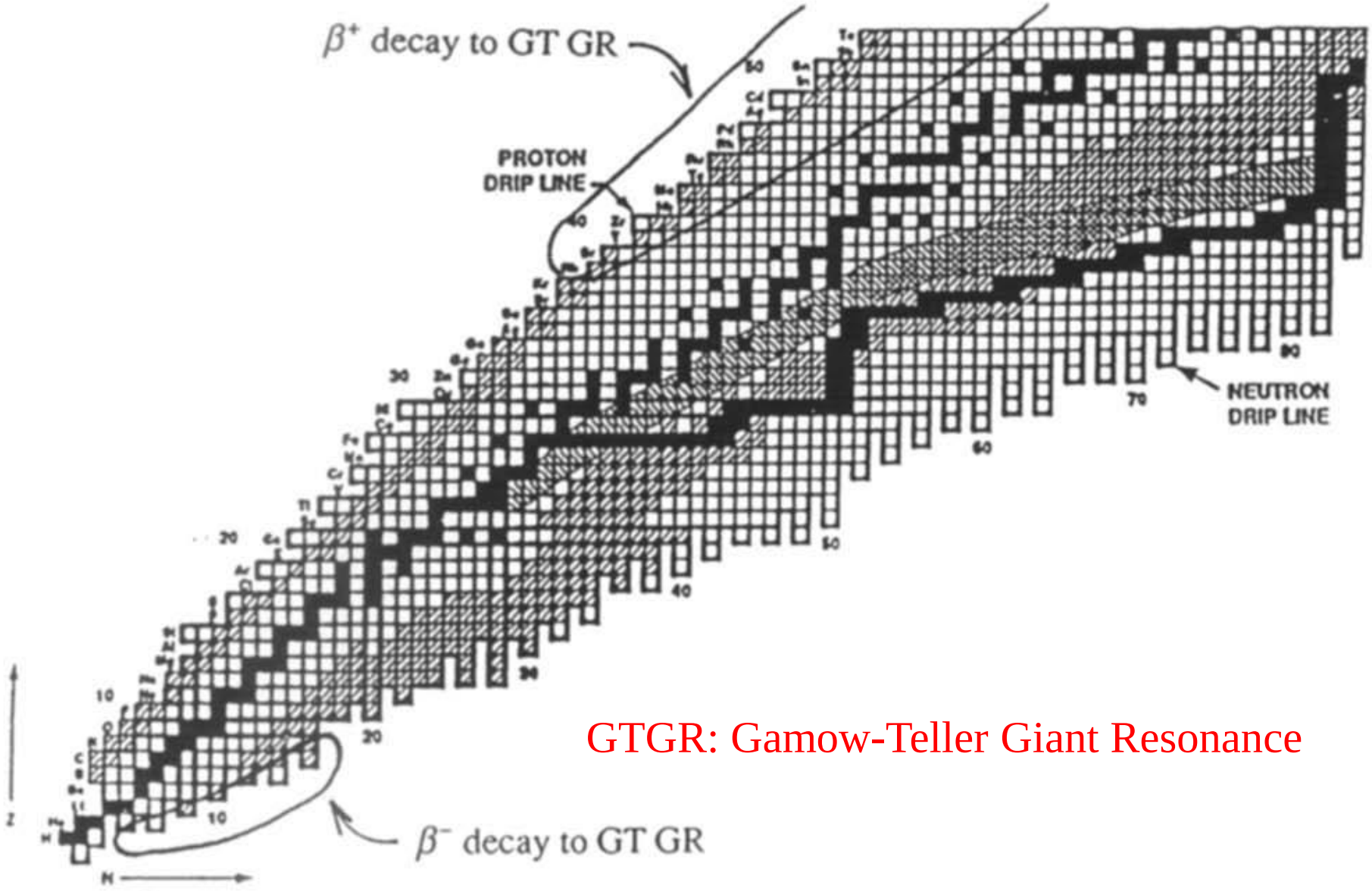

GTGR: Gamow-Teller Giant Resonance

I. Hamamoto, NPA A577 (1994) 19c

The calculated position of $Q_{\beta n}$ window for delayed neutron emission compared to energies of the GT pygmy-resonance (ω_{GT}) and main 0^- transitions ($\omega_{1,2}$) in **Ni isotopes**.

Transition energies and neutron-emission windows are plotted with the opposite sign.

Zero energy corresponds to mothers ground states.

For the lowest energy branch of the 0^- transitions (ω_1), only the points for A = 77–81 are shown.

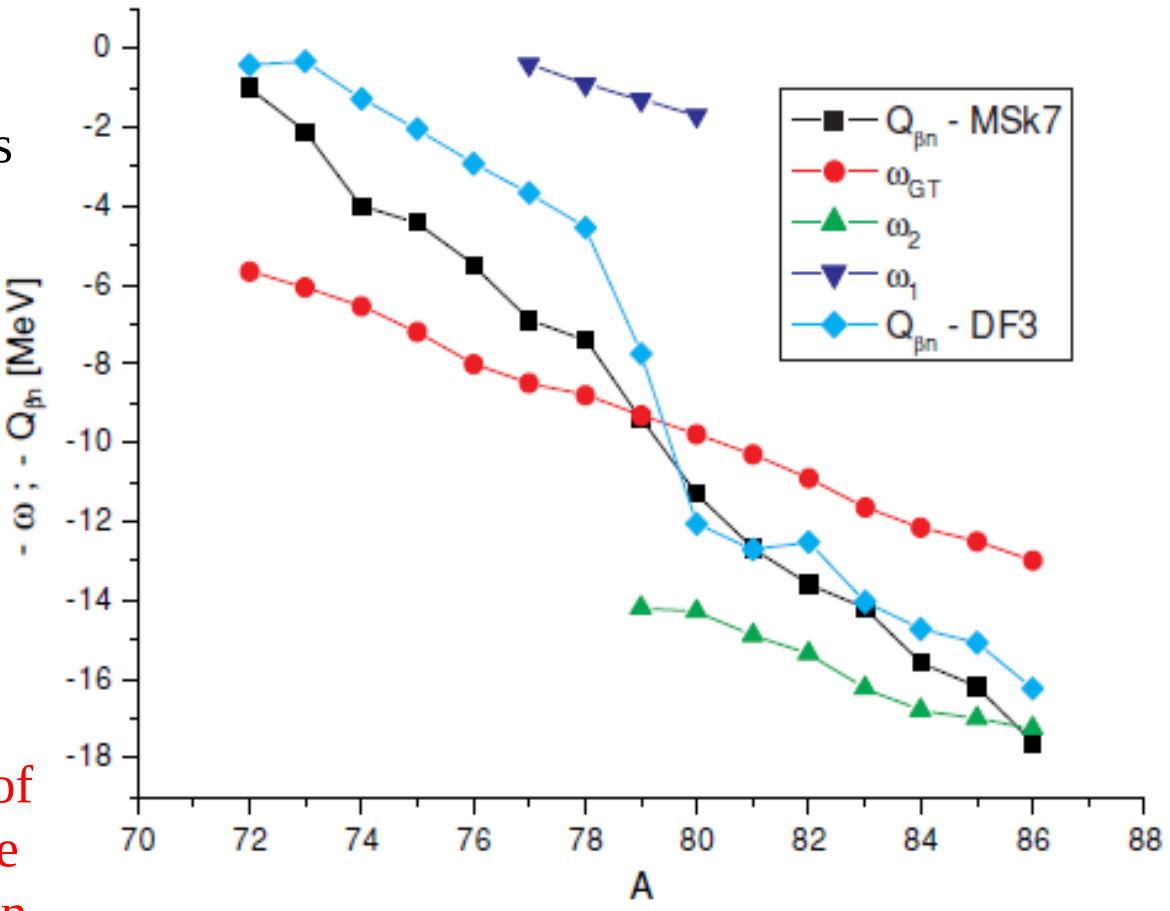

I.N. Borzov, PRC **71** (2005) 065801

(a) Total β-decay half-lives and (b) delayed neutron emission probabilities for Ni isotopes predicted from density functional of Fayans (DF3) + continuum QRPA including the allowed (GT) plus first-forbidden (FF) transitions, and the allowed transitions, in comparison with the Finite-range droplet model (FRDM) + RPA calculation for allowed transitions (Möller) and experimental data a) and b).

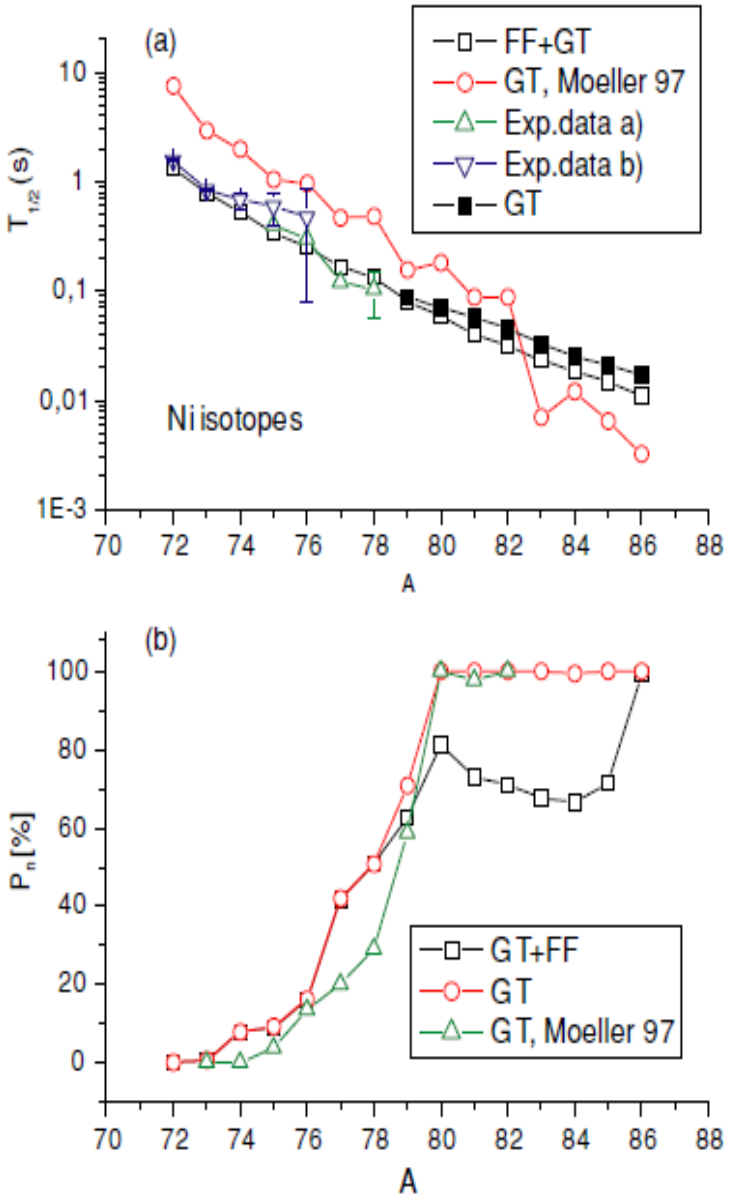

I.N. Borzov, PRC **71** (2005) 065801

Neutron detector BELEN consisting of 48 counters will merge with other neutron detection setups from Japan, Russia, and USA and the AIDA particle detector from the UK into the “BRIKEN” detector to perform experiments at RIKEN in 2015/2016.

BRIKEN collaboration is intending to measure β-delayed neutron emission in the “^{78}Ni and beyond” part of nuclear chart.

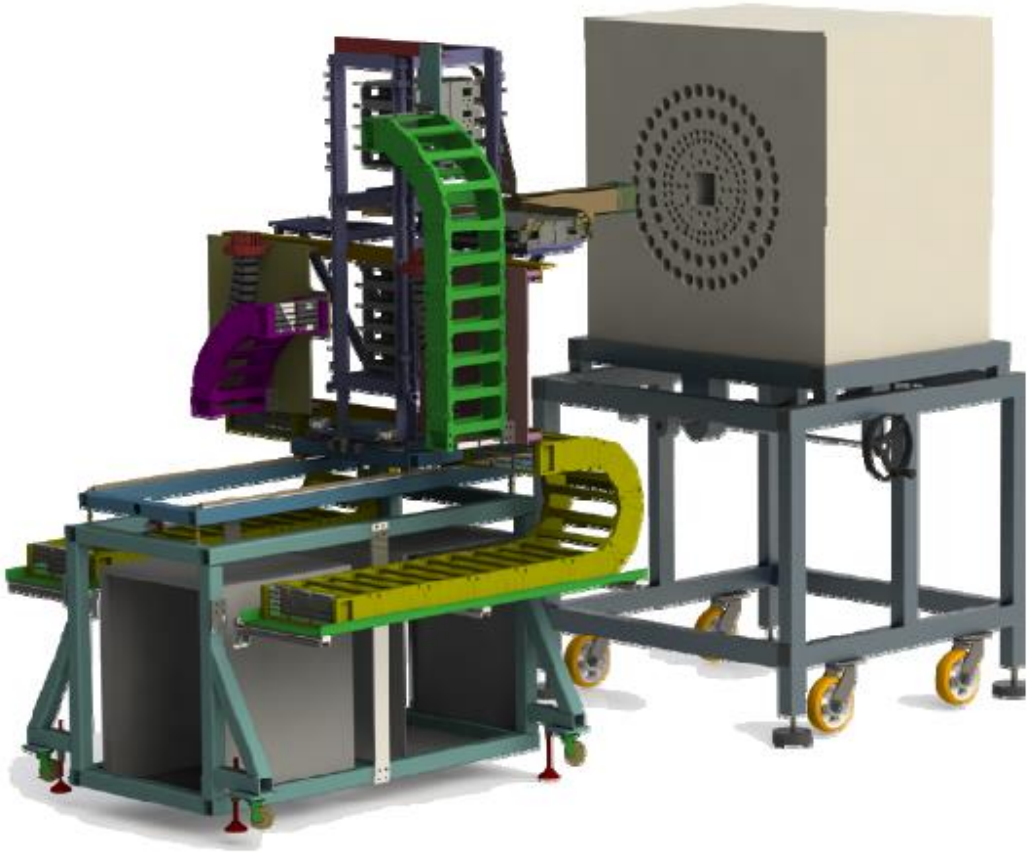

Self-consistent HF-based RPA results for the strength function $S(E)$ distribution of the isoscalar dipole response

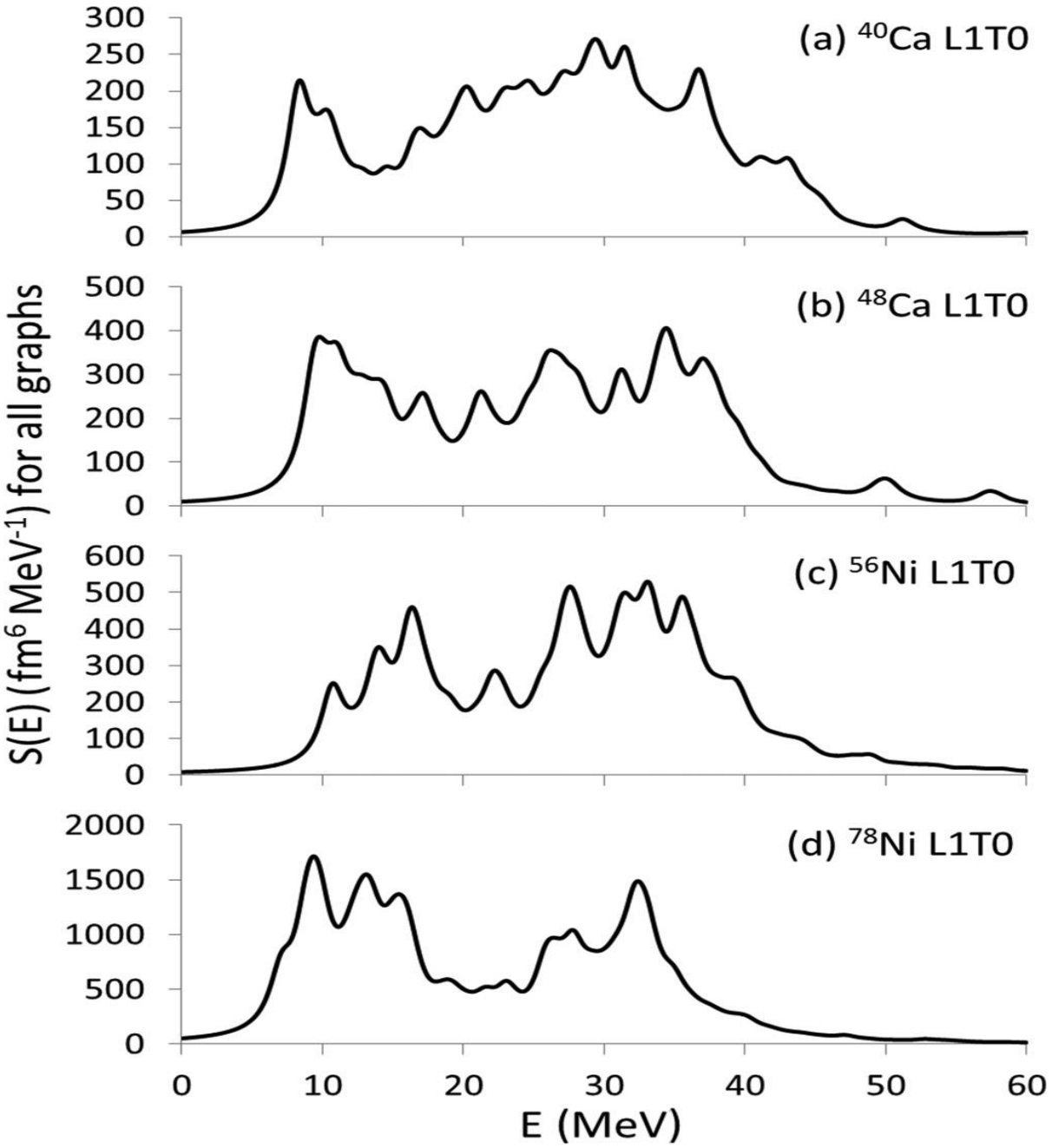

N. Auerbach *et al.*,
PRC **89** (2014) 014335

Self-consistent HF-based RPA results for the strength function $S(E)$ distribution of the isovector dipole response

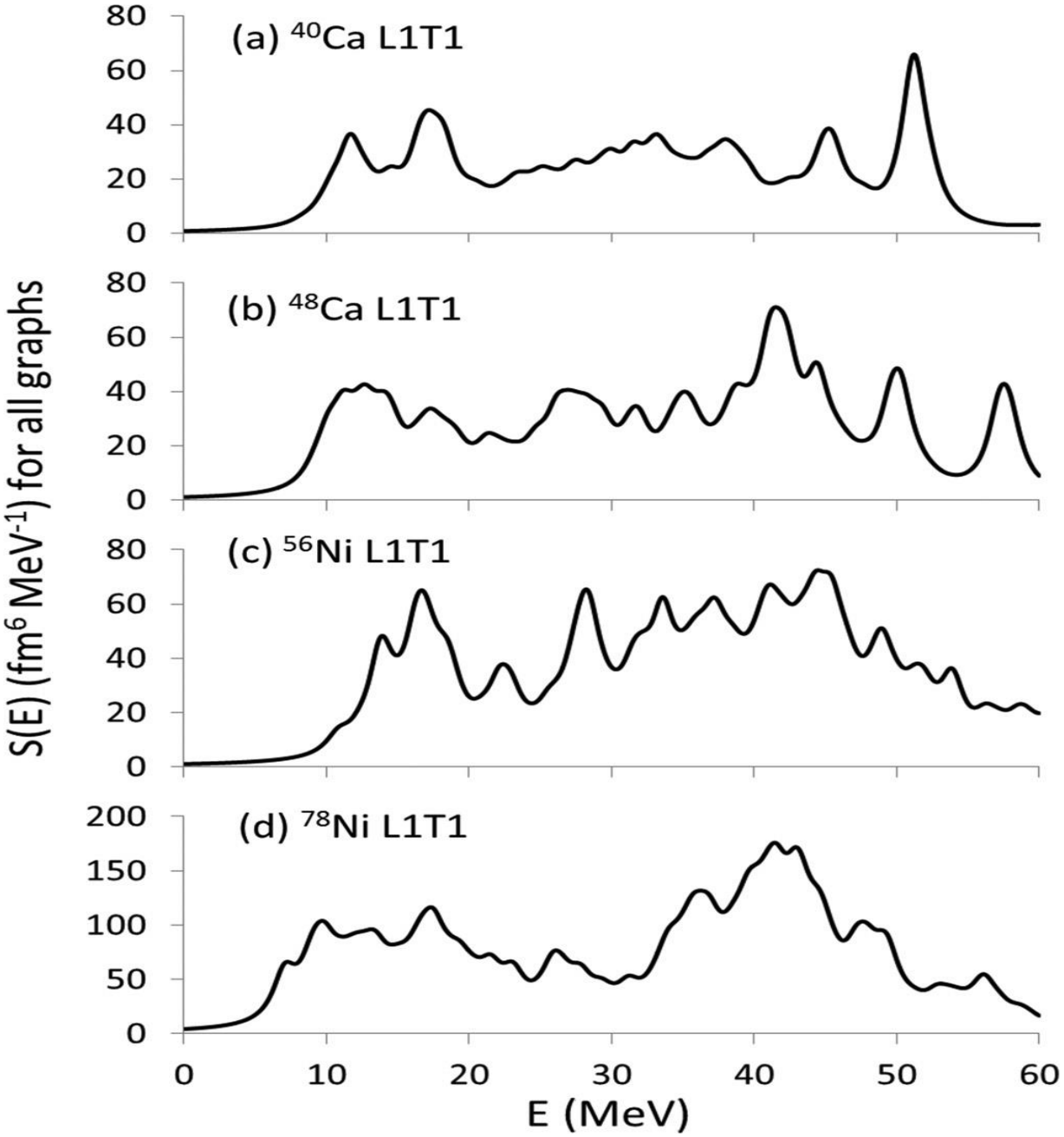

N. Auerbach *et al.*,
PRC **89** (2014) 014335

Distribution of isovector dipole strength for the three closed-(sub)shell nickel isotopes ^{56}Ni, ^{68}Ni, and ^{78}Ni calculated in HF-plus-RPA using the FSUGold interaction parameter set.

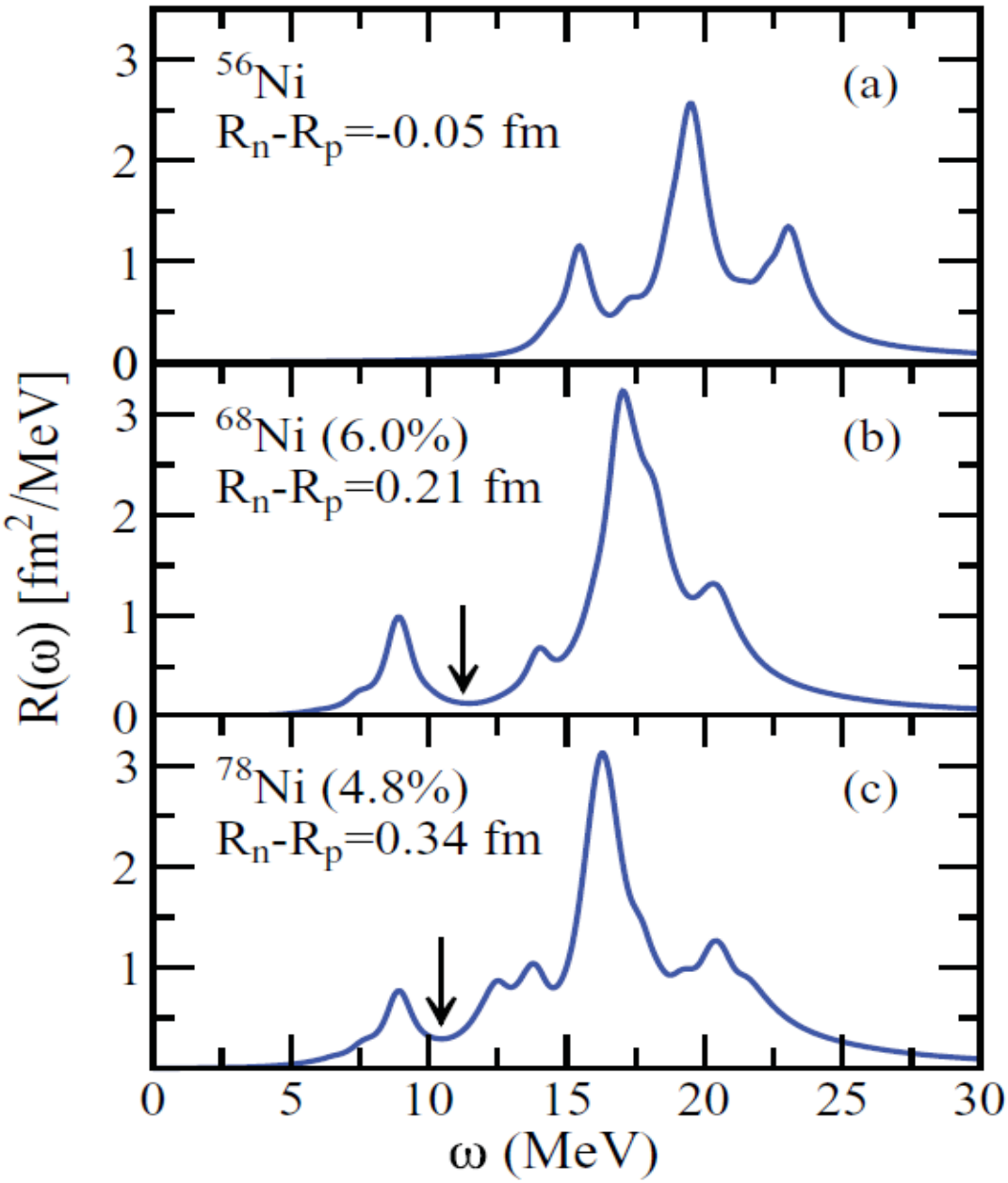

J. Piekarewicz,
PRC **83** (2011) 034319

Isoscalar
(solid, scale on left)
and Isovector
(dashed, scale on right)
1^- strength functions
for even Ni isotopes
(SkM* interaction).

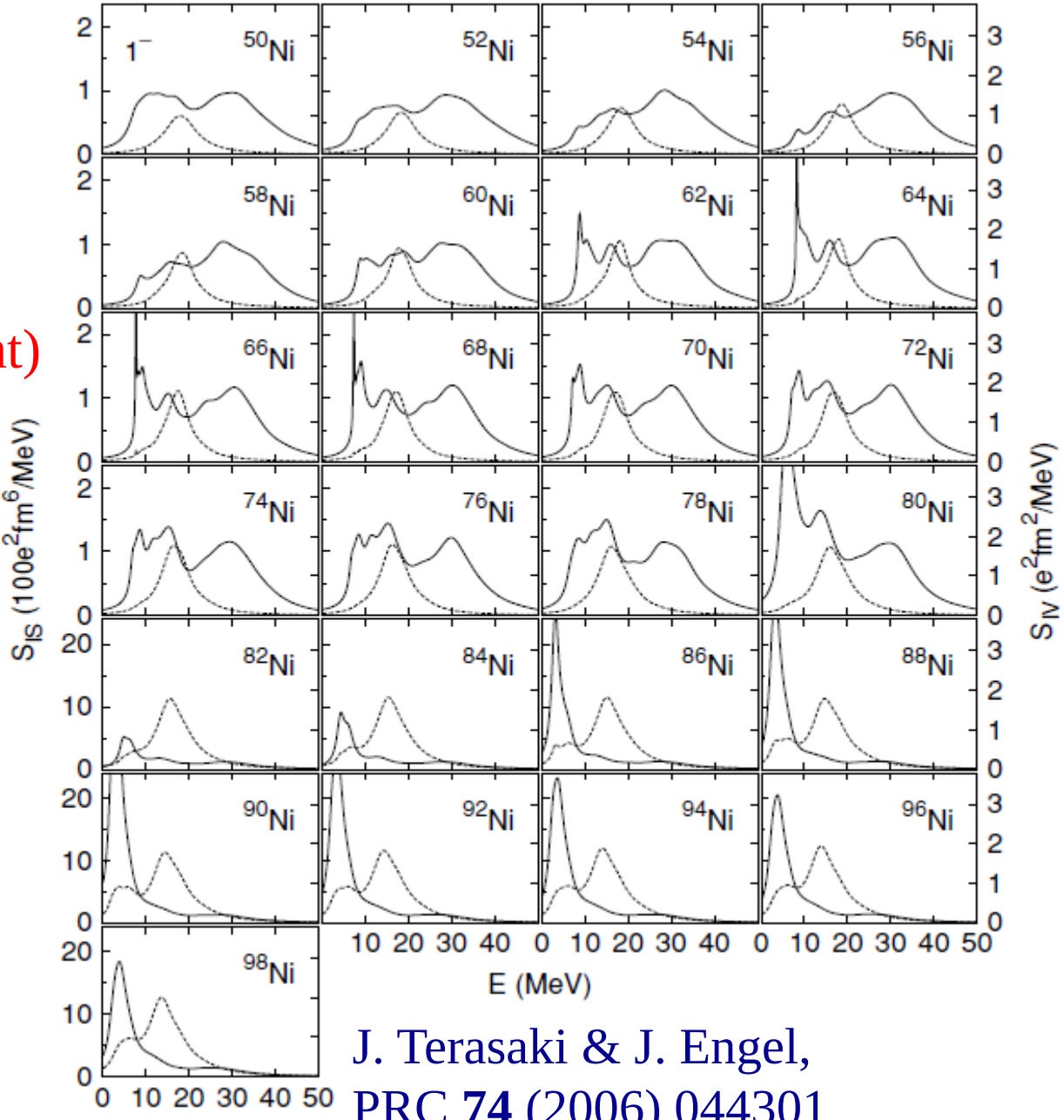

J. Terasaki & J. Engel,
PRC **74** (2006) 044301

Multipole assignment with α–γ angular correlation

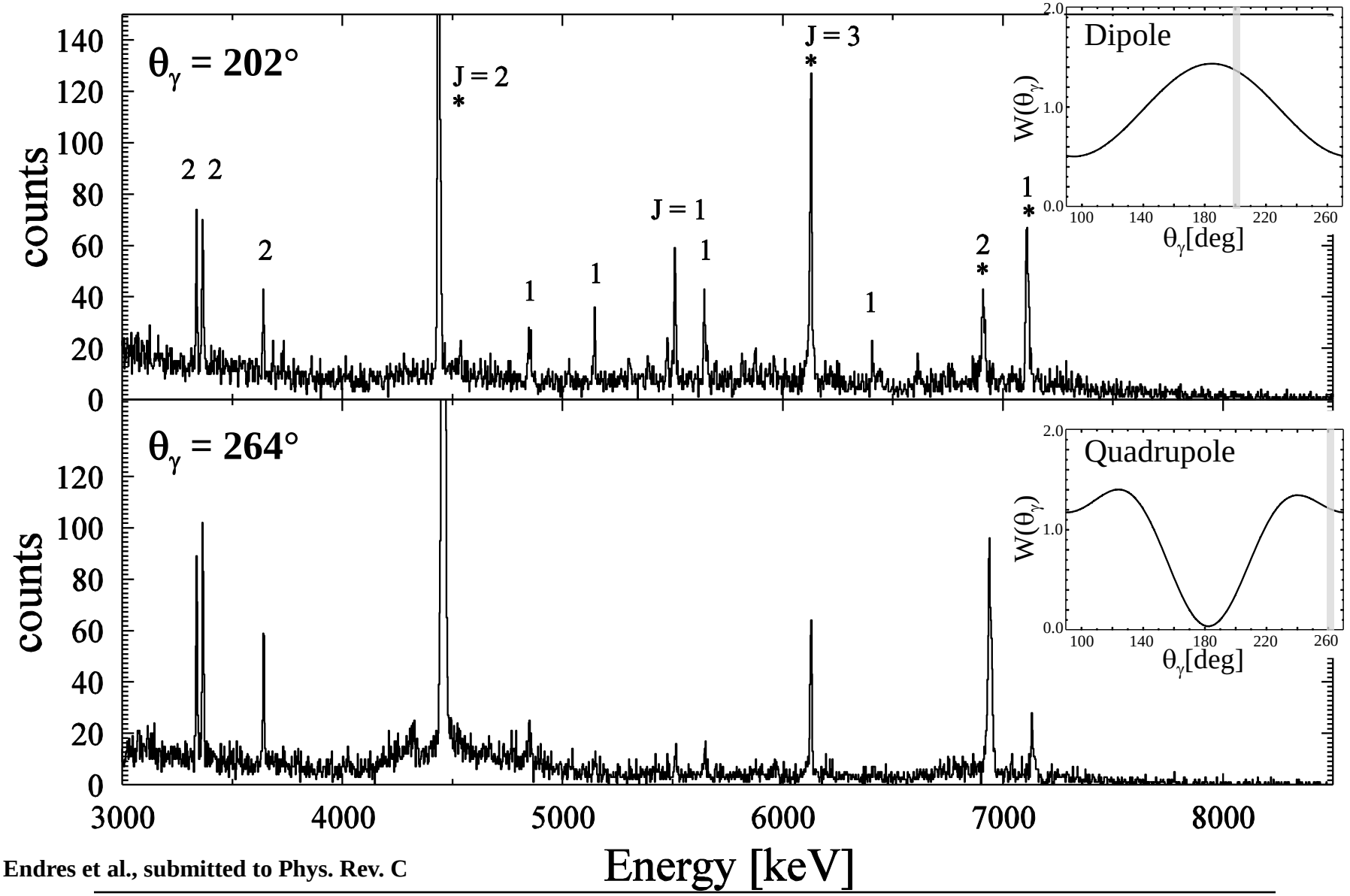

J. Endres et al., submitted to Phys. Rev. C

Multipole assignment with α–γ angular correlation

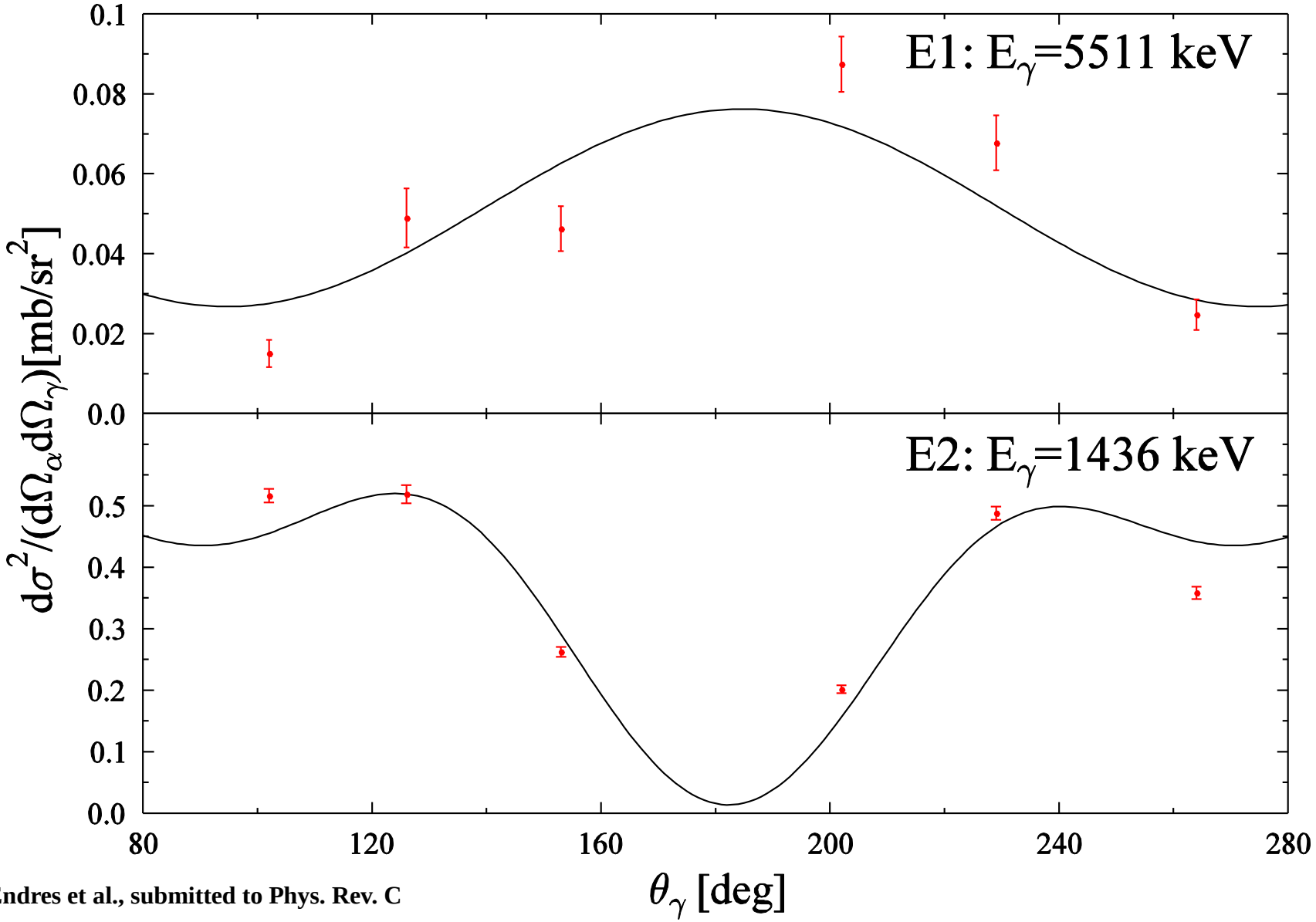

J. Endres et al., submitted to Phys. Rev. C

Comparison of (α,α′γ) with (γ,γ′) on ^{138}Ba

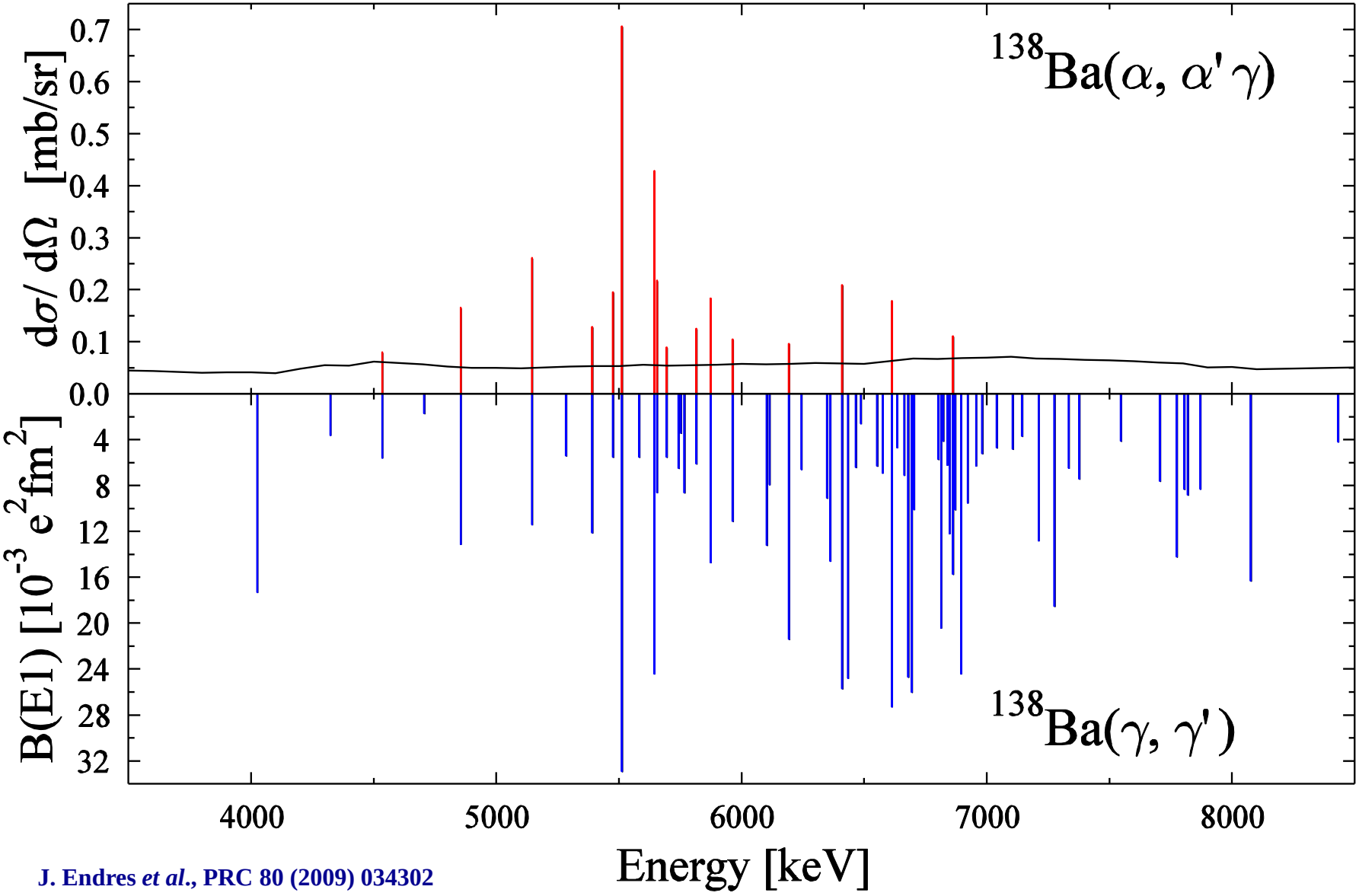

J. Endres *et al.*, PRC 80 (2009) 034302

Systematics

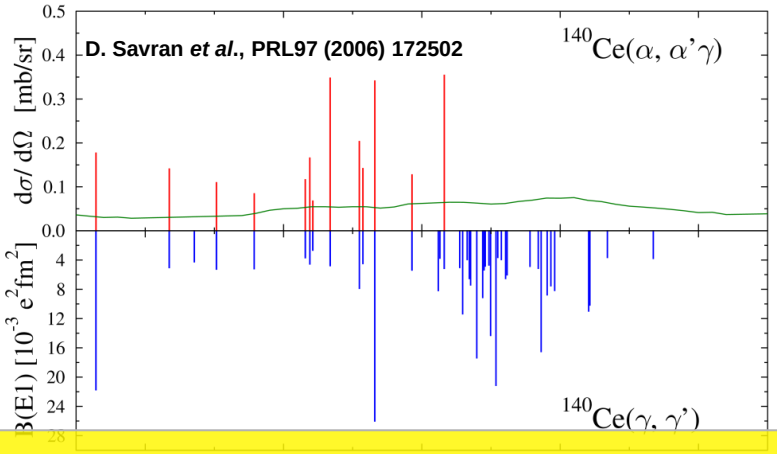

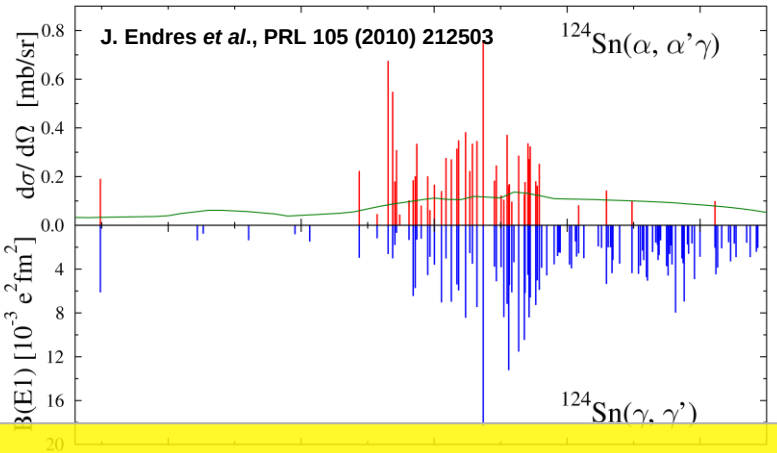

Different response to photons and α-particles points to different underlying structures

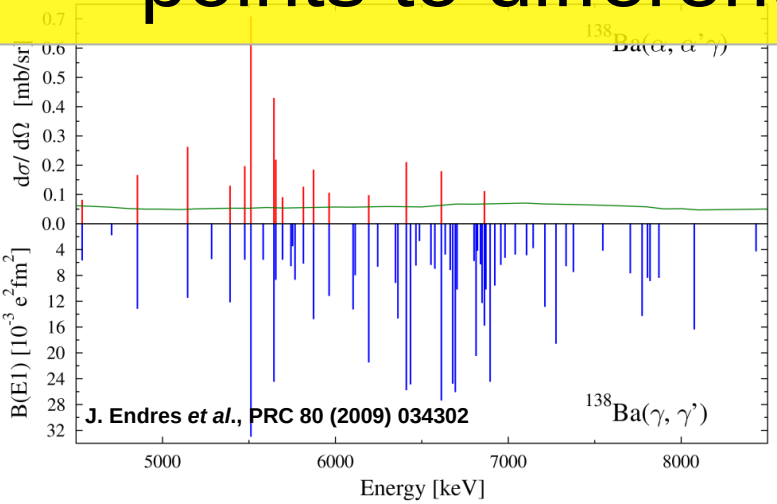

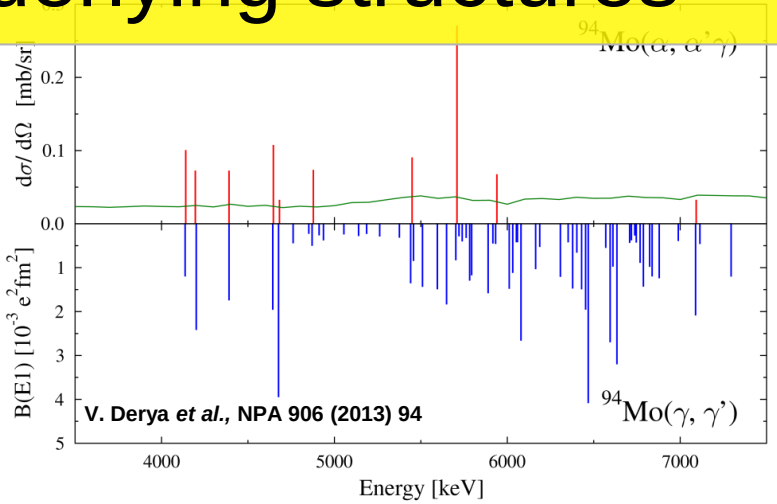

Thank you for your attention